CellPress

Current Biology

Article

An evolutionarily ancient transcription factor drives spore morphogenesis in mushroom-forming fungi

Zhihao Hou,[1,2,6] Zsolt Merényi,[1] Yashu Yang,[3,4] Yan Zhang,[5] Árpád Csernetics,[1] Balázs Bálint,[1] Botond Hegedüs,[1] Csenge Földi,[1,2] Hongli Wu,[1] Zsolt Kristóffy,[1] Edit Ábrahám,[1] Nikolett Miklovics,[1] Máté Virágh,[1] Xiao-Bin Liu,[1] Nikolett Zsibrita,[1] Zoltán Lipinszki,[1] Ildikó Karcagi,[1] Wei Gao,[3,4] and László G. Nagy[1,7,8,*]

[1]Synthetic and Systems Biology Unit, Institute of Biochemistry, HUN-REN Biological Research Centre Szeged, Szeged 6726, Hungary
[2]Doctoral School of Biology, Faculty of Science and Informatics, University of Szeged, Szeged 6726, Hungary
[3]Institute of Agricultural Resources and Regional Planning, Chinese Academy of Agricultural Sciences, Beijing 100081, China
[4]State Key Laboratory of Efficient Utilization of Arid and Semi-Arid Arable Land in Northern China, Beijing 100081, China
[5]College of Plant Protection, Shandong Agricultural University, Taian 271018, China
[6]X (formerly Twitter): @ZhihaoHou
[7]X (formerly Twitter): @laszlognagy
[8]Lead contact
*Correspondence: lnagy@fungenomelab.com
https://doi.org/10.1016/j.cub.2025.02.025

SUMMARY

Sporulation is the most widespread means of reproduction and dispersal in fungi and, at the same time, an industrially important trait in crop mushrooms. In the Basidiomycota, sexual spores are produced on specialized cells known as basidia, from which they are forcibly discharged with the highest known acceleration in nature. However, the genetics of sporulation remains poorly known. Here, we identify a new, highly conserved transcription factor, sporulation-related regulator 1 (*srr1*), and systematically address the genetics of spore formation for the first time in the Basidiomycota. We show that Srr1 regulates postmeiotic spore morphogenesis, but not other aspects of fruiting body development or meiosis, and its role is conserved in the phylogenetically distant, but industrially important, *Pleurotus* spp. (oyster mushrooms). We used RNA sequencing to understand genes directly or indirectly regulated by Srr1 and identified a strongly supported binding motif for the protein. Using an inferred network of putative target genes regulated by Srr1 and comparative genomics, we identified genes lost in secondarily non-ballistosporic taxa, including a novel sporulation-specific chitinase gene. Overall, our study offers systematic insights into the genetics of spore morphogenesis in the Basidiomycota.

INTRODUCTION

Sporulation is one of the most fundamental phases in the fungal life cycle. It is the primary means by which fungi reproduce, disperse to new habitats, survive unfavorable conditions, and, in sexual spores, generate genetic variability for adaptation to new niches. Fungi produce massive amounts of spores, which can reach up to one billion/day for a single fruiting body,[1] that are carried by winds or other vectors to new habitats. In mushroom-forming fungi (Agaricomycetes), air currents generated by the fruiting body can also contribute to lifting spores above ground so that they can travel significant distances from the parent organism.[2] *En masse*, spores pose health hazards and may even contribute to raindrop nucleation.[3,4] During Basidiomycota evolution, sporulation may have been one of the main constraints driving trends and changes in fruiting body morphologies.[5]

Spore formation includes the generation of haploid nuclei, the formation of spores, and their discharge. In the Basidiomycota, spore morphogenesis is best understood in *Coprinopsis cinerea* (*C. cinerea*),[6] commonly known as the ''ink-cap mushroom,'' named after the autolysis of its fruiting bodies,[7] though it has been studied in several other species too.[8–10] It starts after the completion of meiosis, which generates four haploid nuclei that will migrate into the developing spores. Spore morphogenesis has been divided into four stages and starts with the emergence of sterigmata, horn-like projections that serve as the platform for spore development.[6] In the next steps, the spore first grows asymmetrically, then enlarges in all directions equally, paralleled by continuous changes to its wall structure and finally the abscission of the spore from the basidium.

Morphogenesis concludes with forcible discharge, called ballistospory, during which the spore is catapulted away from the basidium by forces generated by the coalescence of a water droplet (Buller's drop) with the spore.[11,12] Ballistospory ensures that spores are shot at considerable distances from the reproductive cell using a powered release mechanism involving estimated initial accelerations exceeding 10,000 g, outpacing all other known rapid movements in nature.[11] The mechanism generating these ultrafast movements has only recently been uncovered.[12–14] Although this has improved our understanding of the physical

laws of spore discharge, the genetics of most steps of spore formation remain unknown. The genetics of meiotic events have been uncovered at some detail, particularly in *C. cinerea*, which has become a model species of meiosis.[15–21] However, the genetics of postmeiotic events, particularly morphogenesis and its regulation, are virtually unknown.

Beyond understanding fungal reproduction, information on the genetics of spore production would also benefit industrial applications and biomedicine. Spores of commercially produced Agaricomycetes, such as *Pleurotus* spp. (oyster mushrooms), can harm technical instrumentation of production facilities,[22] cause respiratory diseases known as mushroom worker's lung, and help strains escape cultivation to establish invasive populations or influence the genetic diversity of natural ones. These problems create a high demand for sporeless mushroom strains. Efforts to produce such strains in industrially relevant fungi,[23] primarily based on mutations in meiotic genes, have yielded industrially accepted sporeless lines.[24–27] However, for identifying novel target genes that can be used in strain improvements programs, uncovering the regulation of spore production is key.

In this study we identified a conserved transcription factor (TF) that regulates spore formation, which we term sporulation-related regulator, Srr1, a C2H2-type zinc-finger TF. By reverse genetic analyses in *C. cinerea* and *Pleurotus cornucopiae* (*P. cornucopiae*), we show that Srr1 has a widely conserved role in regulating postmeiotic events of spore formation. RNA sequencing (RNA-seq) and motif analyses unveiled an Srr1 regulon of ~600 genes and revealed biochemical functions involved in spore formation. Genomic analyses identified genes that, based on expression and presence/absence patterns, are associated with the emergence and loss of ballistospory. This work uncovered a novel regulator of sporogenesis in Basidiomycota and its target genes and provided the first systematic insights into the genes involved in spore morphogenesis.

RESULTS

Srr1 is a novel regulator of sporulation in the Agaricomycetes

For identifying potential regulators of sporulation, we scrutinized genes upregulated in sporulating gill samples of the young fruiting body stage of *C. cinerea*[6] compared with other tissues or other developmental stages, based on data from Krizsán et al.[28] We identified seven genes with an expression peak in gills, of which only one, *C. cinerea* 451915 (JGI Copcin2 proteinID: 2262473, *C. cinerea* Okoyama7#130 CC1G_00038, XP_001836902.2), was exclusively expressed in the gills, with no detectable expression (<10 counts per million [CPM]) in all other tissues and developmental stages (Figure S1A). *C. cinerea* 451915 also had the highest fold-change compared with the average expression in all stages (Figure S1B) and follows a gill-specific expression pattern in other basidiomycetes too, such as *Laccaria bicolor*, *Cyclocybe aegerita*, and *Pleurotus ostreatus* (Figures S1C–S1E), based on published data.[29–31]

We generated a knockout mutant for this gene in the self-compatible *C. cinerea* A43mutB43mut #326 pab1-1 strain, using a ribonucleoprotein (RNP) complex.[32] We targeted the locus with two RNPs to generate a 1,666-base pair (bp) deletion (Figure S2B). The genotypes of the knockout mutant were confirmed by PCR using diagnostic primer pairs and RT-PCR to verify the lack of expression of the target gene (Figures S2C–S2E).

The 451915 knockout mutants displayed no phenotypic difference with the wild type (WT) in the vegetative mycelium, oidiation capacity, or early stages of fruiting body development (Figures 1A, S2F, and S2G). Mature fruiting bodies, in contrast, had white caps, indicative of a failure to produce black spores (Figure 1A; Video S1). Gills, cystidia, and pseudoparaphyzes did not differ from the WT, and the autolytic process typical of *Coprinopsis* was also similar to that of the WT (Figures 1A and 1B). In the mutant, spore development is arrested at the stage when spore initials emerge at the sterigma tips (Figure 1C), corresponding to stage one or two, as defined in *C. cinerea*.[6] In the mutant, these spore initials could not inflate further to reach a final spore shape and size. Fluorescent microscopy indicated that the basidia of the mutant contained four nuclei (Figure 1C), indicative of successful completion of meiosis. These findings indicate that the mutants show a postmeiotic arrest in spore development, suggesting that 451915 regulates morphogenetic processes following meiosis, such as spore initiation, spore enlargement, nuclei migration, and spore discharge. Hereafter, we refer to *C. cinerea* 451915 as sporulation-related regulator 1, *srr1*. *srr1* encodes a 684-amino acid (aa) polypeptide that contains three C2H2-type zinc-finger domains (Figure S2H), indicating it is a TF of the C2H2-type zinc-finger family. Together, these data indicate that Srr1 is a novel TF with specific postmeiotic roles in sporulation.

Srr1 is conserved across Agaricomycetes

To assess the distribution of Srr1 orthologs in the Agaricomycetes, we inferred a maximum likelihood gene tree for homologs of *C. cinerea* Srr1 identified in 189 whole genomes using BLASTP (E value < 10^{-10}). Orthologs of Srr1 were defined as the most inclusive clade of the gene tree that does not comprise deep duplications. Our results indicate that Srr1 is widely conserved in the Agaricomycetes (Figures 2A and 2B), with clear orthologs in the Agaricales, Atheliales, Boletales, Amylocorticiales, Polyporales, Jaapiales, Russulales, and Gloeophyllales but missing in other Agaricomycetes orders (Figures 2A and 2B). This suggests that Srr1 evolved in the most recent common ancestor of the Russulales and more-derived Agaricomycetes. Within the Agaricales, the gene is conserved, except in the Schizophyllineae and Marasmiineae suborders, which lack orthologs due to gene losses. We found that Srr1 is a single-copy gene in most species that possess it, with few exceptions of recent duplications (e.g., *Suillus luteus*, see Figure 2B).

The protein sequence shows overall low conservation, except for the three consecutive C2H2-type DNA-binding-domain regions and an ~50 aa upstream region, which are highly conserved and show a characteristic sequence signature that differs from that of other C2H2 families (Figures 2C and 2D)

Outside Agaricomycetes, Srr1 did not have orthologs based on searches with the complete protein sequence. However, BLAST analysis of the DNA-binding-domain region (572–657 in the polypeptide) revealed highest similarity to Mld-1 of *Neurospora crassa*, which is involved in melanin production.[33]

Conserved role in oyster mushrooms

The phylogenetic analyses of the Srr1 family revealed the presence of orthologs in the genus *Pleurotus*, which includes some

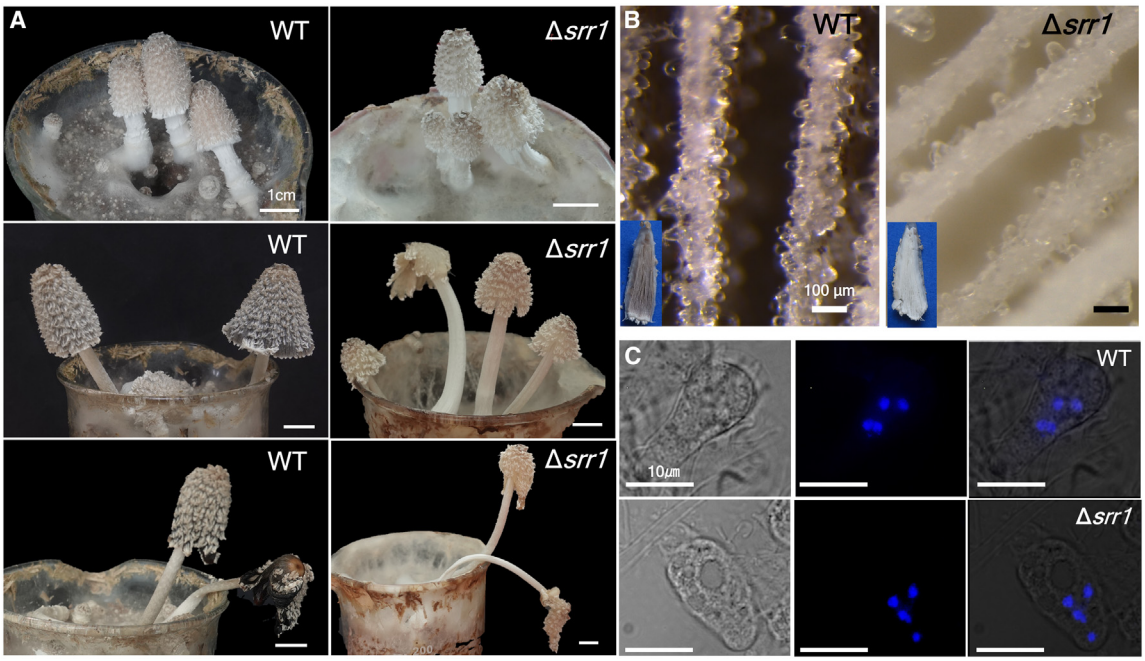

Figure 1. Phenotypic comparison of fruiting bodies, gills, and basidia of Δ*srr1* and wild-type strains

(A) Fruiting bodies at different developmental stages.

(B) Stereomicroscope images of the gill showing the cystidia and pseudoparaphyzes and the picture on the left corner showing the stages of the sampled gill for stereomicroscopy.

(C) Fluorescent microscope images showing the number of nuclei in the basidia using Hoechst staining.

See also Figures S1 and S2 and Video S1.

of the most widely cultivated mushrooms worldwide. Based on previously published transcriptome data, the Srr1 orthologous gene of *P. ostreatus* was upregulated in gills.[29]

To analyze the role of the Srr1 orthologs in this genus, we used *P. cornucopiae* in which RNA interference (RNAi) has been established, to silence the g1654 gene (Plecor_9219244 in Figure 2B). An RNAi-1654 vector was transformed into the WT strain CCMSSC00406 as the host. Quantitative PCR (qPCR) indicated that, compared with the WT strain, the expression level of g1654 in the gills of RNAi-g1654-4 and RNAi-g1654-14 strains decreased by 33.92% and 35.61%, respectively (Figure 3A). These two strains were selected for subsequent experiments.

Fruiting experiments were conducted with RNAi-g1654-4, RNAi-g1654-14, and the WT 406 strain. Compared with the WT strain, RNAi strains had nearly identical fruiting bodies (Figure S3B). The spore prints of the RNAi strains were noticeably thinner and lighter in color (Figure 3B). In line with these results, spore quantity was significantly reduced in the RNAi-g1654-4 and RNAi-g1654-14 strains compared with the WT strain (Figure 3C). These results suggest that g1654 plays a role in spore formation in *P. cornucopiae*, and its reduced expression can explain the lower quantity of spores in RNAi strains.

RNA-seq reveals that Srr1 is mostly an activator

The sporulation process of *C. cinerea* Δ*srr1* mutant stopped after the meiosis, when spore initials emerge at the sterigma tips. For understanding what genes Srr1 regulates, we sampled the gills of the WT and Δ*srr1*, at the time point when sporogenesis of Δ*srr1* mutants stopped, for RNA-seq (Figure 4A). Pearson correlation coefficients showed good grouping for both WT and Δ*srr1* replicates (Figure S4A). By analyzing differentially expressed genes (DEGs, $p \leq 0.05$, |fold-change (FC)| ≥ 2) we identified 154 and 559 genes that were significantly upregulated and downregulated, respectively, in the Δ*srr1* strain compared with WT (Figure 4B; Data S1A and S1B). The higher number of downregulated genes (559) compared with upregulated genes (154) suggests that Srr1 is probably an activator, though DEGs likely include both direct and indirect targets. By cross-checking the expression level of downregulated DEGs with data from Krizsán et al.,[28] we found that these genes show a significant enrichment among gill (YFB_L) upregulated genes (Fisher's Exact Test [FET], p value = 4.17×10^{-64}) (Figure 4C), indicating that these genes become active in the gill during sporogenesis.

To characterize the functions of downregulated DEGs, we used GO and KEGG enrichment analysis. Overall, a significantly lower ratio (FET, $p = 3.69 \times 10^{-12}$ to 4.16×10^{-4}) of downregulated DEGs have associated GO terms (Data S2A) than all genes in the genome, indicating that the functions of sporulation-related DEGs are particularly poorly known relative to the genome-wide average in *C. cinerea*. Nevertheless, we identified 103 significantly enriched GO terms (hypergeometric test, $p < 0.05$) (Figure S4B; Data S2B). We found that enriched GO terms can be grouped into broad categories, corresponding to the fungal cell wall, amino acid biosynthesis, TORC signaling, sugar metabolism, and extracellular space (Data S2B; Table S1). Here, we discuss these gene groups in detail.

The fungal cell wall consists of glucans, chitin and mannans, and sometimes lipids, whereas the spore wall of *C. cinerea* additionally

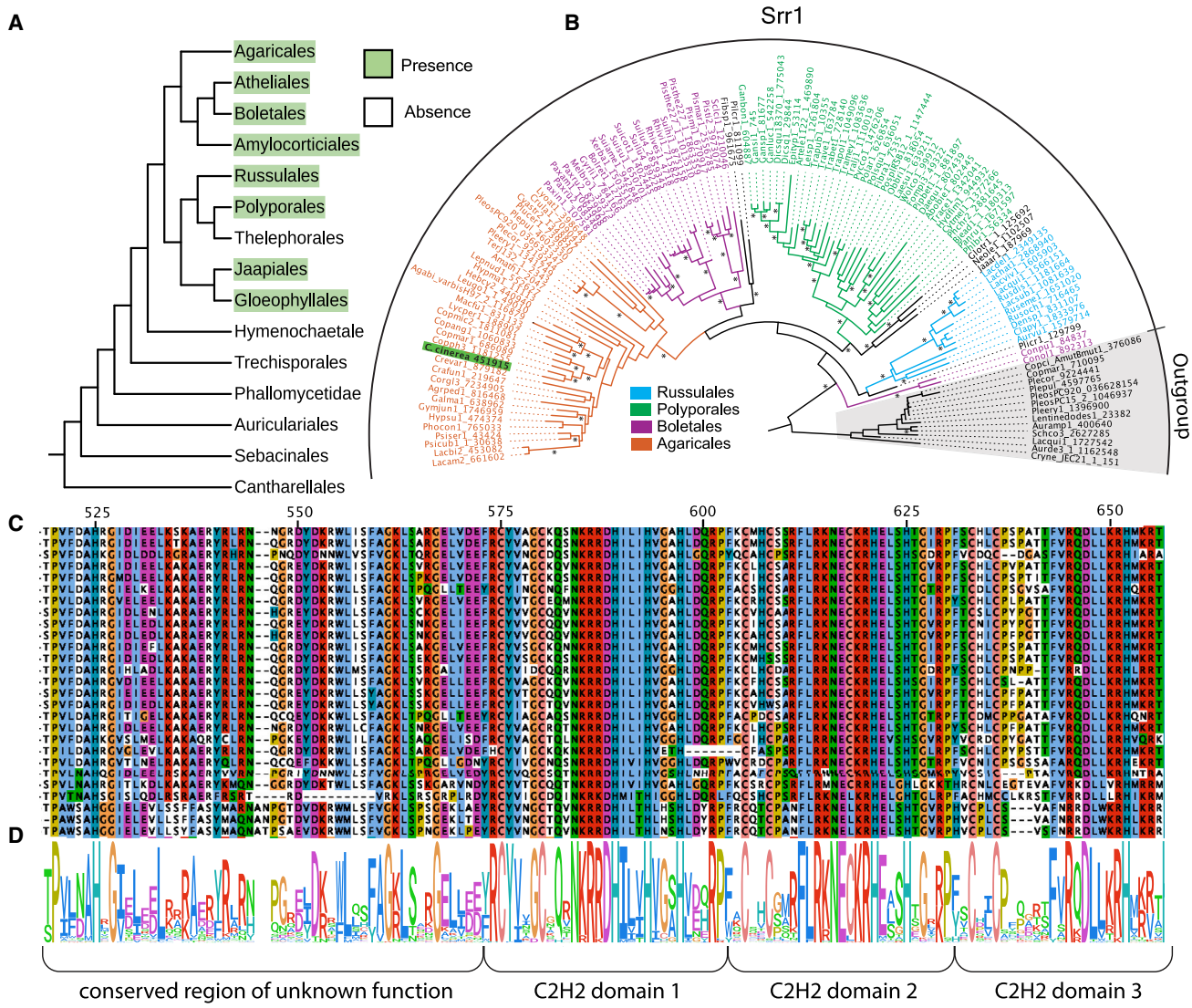

Figure 2. Evolutionary conservation of Srr1 across mushroom-forming fungi

(A) Schematic tree showing the presence or absence of Srr1 in Agaricomycetes.

(B) Maximum likelihood gene tree of Srr1 orthologs and homologs. Asterisk marks branches with >70% bootstrap support.

(C) The conservation of DNA-binding domains and flanking regions of unknown function in the Srr1 polypeptide. Multiple sequence alignment shown only for the Agaricales.

(D) Sequence logos (bit scaled) of position-wise residue conservation in the DNA-binding domains of Srr1 orthologs.

contains melanin and has multiple layers that change dynamically during spore development.[6,34] We assigned fungal cell wall (FCW)-related genes by GO and manual annotation of *C. cinerea* cell wall genes from previous study.[35] These encode both cell wall synthetic and modifying enzymes, including two chitin synthases, four associated with chitin remodeling, seven with glucan remodeling/assembly, three with mannan remodeling, and one encoding a putative alginate lyase (Figure S4C; Table S1). These results suggest that fungal cell wall remodeling may be regulated by Srr1 during sporulation. Because Δ*srr1* strains displayed normal deliquescence and gill cell morphology, we speculate that the downregulated fungal-cell-wall-related genes are involved in spore morphogenesis or abscission.

The next group of 22 enriched GO terms is linked to aromatic amino acid (AAA) biosynthesis (Figure S4D; Table S1; Data S2B). A KEGG pathway enrichment also shows that biosynthesis of amino acids, and phenylalanine, tyrosine, and tryptophan biosynthesis, is significantly enriched among downregulated DEGs (Data S2C). These terms correspond to seven genes, five involved in AAA biosynthesis, one in histidine biosynthesis, and one in arginine biosynthesis (Figure S4D; Data S2D). Six of the seven genes are specifically upregulated in the young fruiting body gills in WT (exception: 493061).[28] These data suggest that the synthesis of AAAs is downregulated in the Δ*srr1* strain. Because the synthesis of other amino acids seems less affected in Δ*srr1*, and as AAAs are the precursors of melanin synthesis,

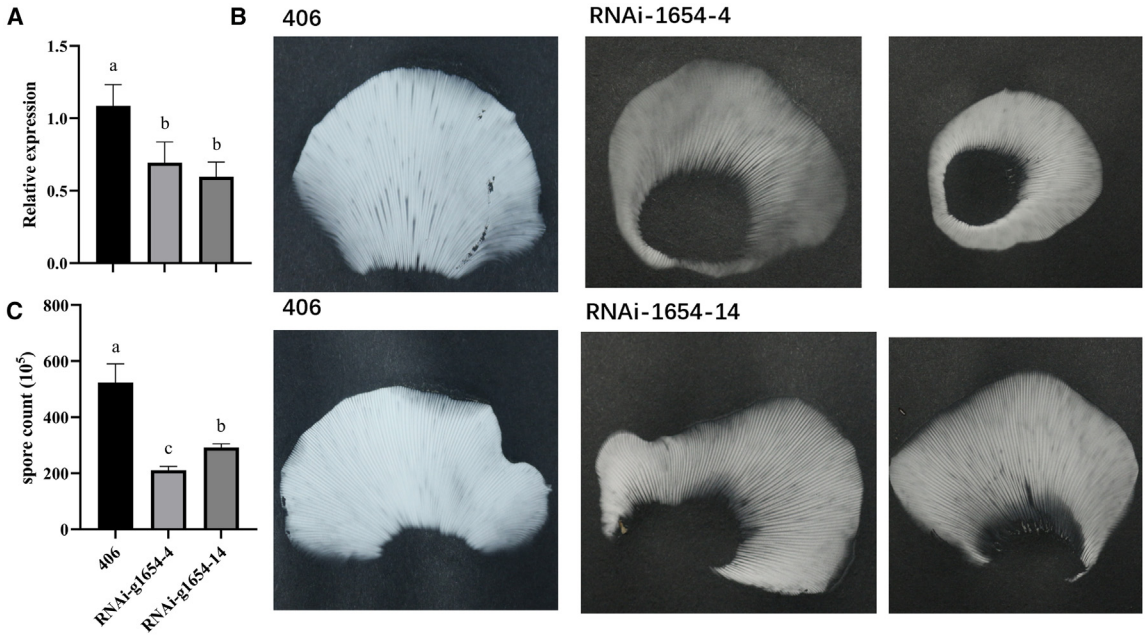

Figure 3. Comparison of *P. cornucopiae srr1* (g1654) expression and spore quantification between silencing and wild-type (406) strains

(A) qPCR expression levels in gills of WT and RNAi lines. Variance among biological replicates is shown.

(B) Spore prints of WT and the 1654-4 and 1654-14 RNAi lines.

(C) Spore counts obtained from 0.5 × 0.5 cm cuttings of spore prints from (B) from WT and two RNAi lines. Significance groups are indicated by letters and variance is indicated.

See also Figure S3.

which,[36] in *C. cinerea*, happens only in spores, we hypothesize that their downregulation may be related to the lack of melanized black spores in the mutant.

The next functional category includes three genes linked to seven GO terms related to target of rapamycin (TOR) (Data S2B). Two genes are upstream of the TORC1 complex, whereas one is part of TORC2 complex (Figure S4E; Table S1). As TORC1 and TORC2 are involved in the regulation of diverse cellular processes (including autophagy and cytokinesis in yeasts) and responses to nutrient availability (e.g., amino acids), it is hard to speculate what their downregulation in our data means for sporogenesis. However, considering the strong signal for amino acid biosynthesis among downregulated DEGs, it is possible that the downregulation of TOR pathway components may be related to the amino acid deficiency that conceivably emerges in the Δ*srr1* mutant. Alternatively, during yeast cytokinesis, the TORC2 complex regulates actomyosin ring constriction,[37] which may also be relevant during sporulation.

The enrichment of the term extracellular region (Data S2B) suggests that extracellular and/or secreted proteins may be affected in the Δ*srr1* strain. We found that downregulated DEGs that encode secreted proteins (88 DEGs, 15.74%) are significantly enriched (FET, $p = 4.74 \times 10^{-7}$) among DEGs compared with the whole genome (8.96%, 1,220/13,615) (Figure 4C; Data S1B). DEGs encoding secreted proteins covered predicted peptidases, fasciclins, cutinases, putatively glucan-related cellulose-binding domains (CBM1), and lysozymes, among others (Data S1B). Previous studies revealed that the endoplasmic reticulum (ER) and Golgi vesicles were becoming active during spore formation in *C. cinerea*.[6,7] This, combined with our results, suggests an increased biosynthesis of secreted proteins during sporulation, potentially to fulfill functions in cell wall remodeling, adhesion, or defense, among others.

Finally, we identified GO terms related to carbohydrate metabolic processes that correspond to malic enzymes of *C. cinerea*. All three malic enzymes (380777, 273609, and 497233) encoded by the genome of this species were downregulated in the Δ*srr1* strain. Although this appears to be a strong signal, its relationship to sporulation is currently obscure, as malic enzymes catalyze the oxidative decarboxylation of malate to pyruvate and, as such, are involved in primary metabolism.

To approximate the downstream transcriptional network of Srr1, we identified transcriptional regulators downregulated in the mutant and found seven TFs (Figure 4D; Data S1B).

Motif and network analyses highlight putative target genes of Srr1

Experimental approaches for screening transcription-factor-binding motifs, such as chromatin immunoprecipitation sequencing (ChIP-seq), are not yet well established in *C. cinerea*. Therefore, to better understand gene regulation by Srr1, we performed bioinformatics-based motif analyses of downregulated genes. Considering the uncertainty in defining *C. cinerea* promoters and regulatory functions of promoter-proximal introns,[38] we first created six promoter datasets with different lengths (300 bp, 500 bp, and intergenic region with first intron) upstream of the start codon for both fold-change two (FC2, 558 genes) and fold-change four (FC4, 266 genes) downregulated genes (excluding *srr1*) (Figure 5A). We

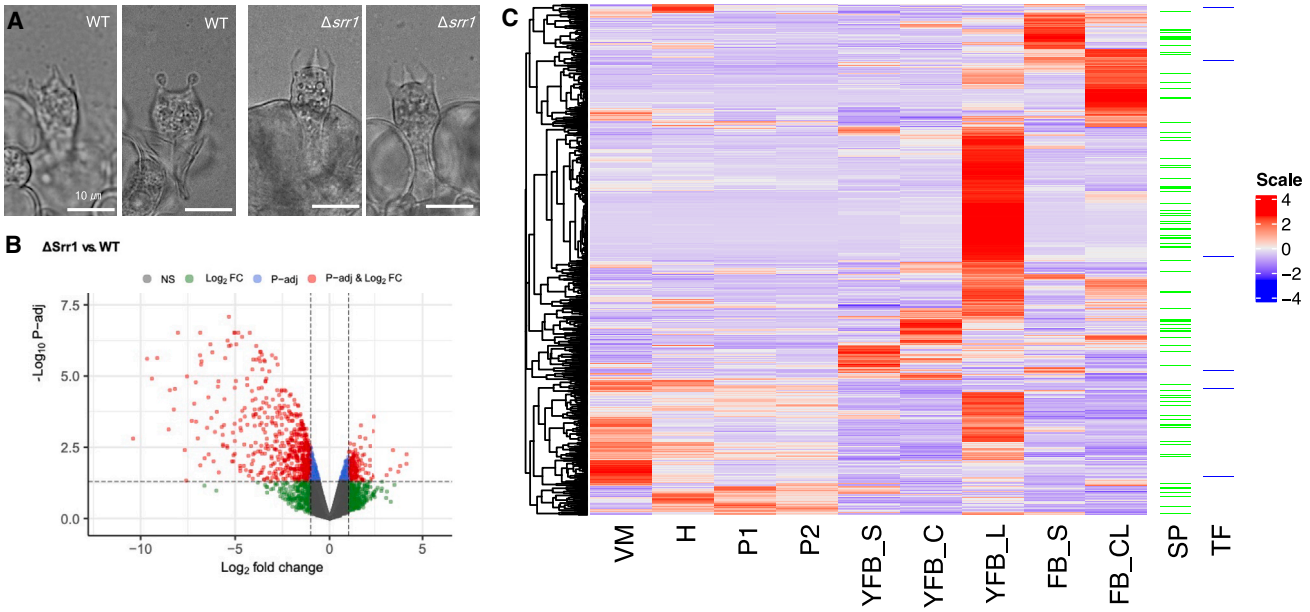

Figure 4. RNA-seq analysis of Δ*srr1*

(A) RNA-seq sampling points of the Δ*srr1* and WT.

(B) Volcano plot of the DEGs.

(C) Heatmap showing the expression of 599 FC_2 down-DEGs in Krizsán et al.'s dataset[28]; note the higher expression of many genes in young fruiting body gills (YFB_L). The abbreviations of different stages are listed in Data S1B. SP, secreted protein; TF, transcription factor. Genes were clustered by the complete linkage method based on Euclidean distance using the scaled *Z* score of CPM values.

See also Figure S4 and Table S1 and Data S1 and S2.

inferred motifs using STREME for these six datasets. We obtained significantly enriched ($p < 0.05$, Binomial test) motif(s) for each of the tested datasets, with variants of one motif, GTGGCTGAC, appearing in all six (Figures 5B and S5A; Data S3B). This indicates that the identification of this motif is robust to different choices in our definition of the promoter sequences. The variants of motif were found in the promoters of 106–260 (27.06–46.99%) genes among different datasets with significantly higher occurrence (FET, $p < 0.05$) compared with the whole genome (Figure 5B; Data S3B). Because a motif found in DEGs may relate to either Srr1 or another TF, we also predicted the binding motif of Srr1 by an independent predictor,[39] which only uses information from the protein sequence of Srr1. We obtained a very similar motif (GTGGCDHWG, Figure 5C), which we interpret as robust support for the identified motif being the binding sequence of Srr1.

For further analyses, we chose the dataset comprising 558 downregulated genes (FC $\geq$ 2), the whole intergenic region upstream of the gene plus the first intron (Down_FC2_Intergenic_first_intron). In this dataset, 260 of the 558 genes contained at least one occurrence of the inferred motif. The distribution of the motif in the promoters is shown in Figure S5B.

For understanding the gene regulatory network of Srr1, we compiled available evidence of potential upstream factors and inferred regulatory relationship into a hypothetical gene regulatory network (Figure 5D). In addition to *srr1*, we identified six other gill-upregulated TFs (Figure S1A). Because none of them were differentially expressed in the Δ*srr1* strain, we hypothesize that some or all of them act upstream of *srr1*, possibly in combination with other signals (Figure 5D). It is possible that activation of *srr1* is linked to the completion of cell-cycle events after meiosis. Downstream of Srr1, our motif analyses identified two downregulated TFs (447714 and 467166) that have the predicted Srr1-binding motif in their promoters and are thus putative direct targets of Srr1 (Data S3B). Another five downregulated TF genes had no Srr1 motif in their promoters, hence we infer they are not directly regulated by Srr1. Both direct and non-direct TFs may regulate the downstream genes, including those associated with the fungal cell wall, AAA synthesis, secreted proteins, and TOR signaling (Figure 5D).

Taken together, our analyses provided a clear signal for the putative binding motif of Srr1 and allowed approximating its regulon in *C. cinerea*. By integrating the available information, we propose a hypothetical regulatory network in which Srr1 acts as a key factor triggered by upstream TFs or signals and regulates the downstream targets to participate in sporogenesis and ballistospory.

Comparative genomics of putative Srr1 targets reveals a link to ballistospory

The forcible discharge of spores occurs after spore formation, and thus its regulation is probably downstream of Srr1. Here, we attempted to gain insights into the genetics of ballistospory by using information from the Δ*srr1* mutant and phylostratigraphic analyses of a 189-genome dataset. This comprised 155 ballistosporic species and 20 that lost ballistospory (henceforth secondarily non-ballistosporic), such as puffballs, bird's nest fungi, and false truffles, as well as seven Ascomycota as outgroups. We searched for gene orthogroups whose presence/absence and origins

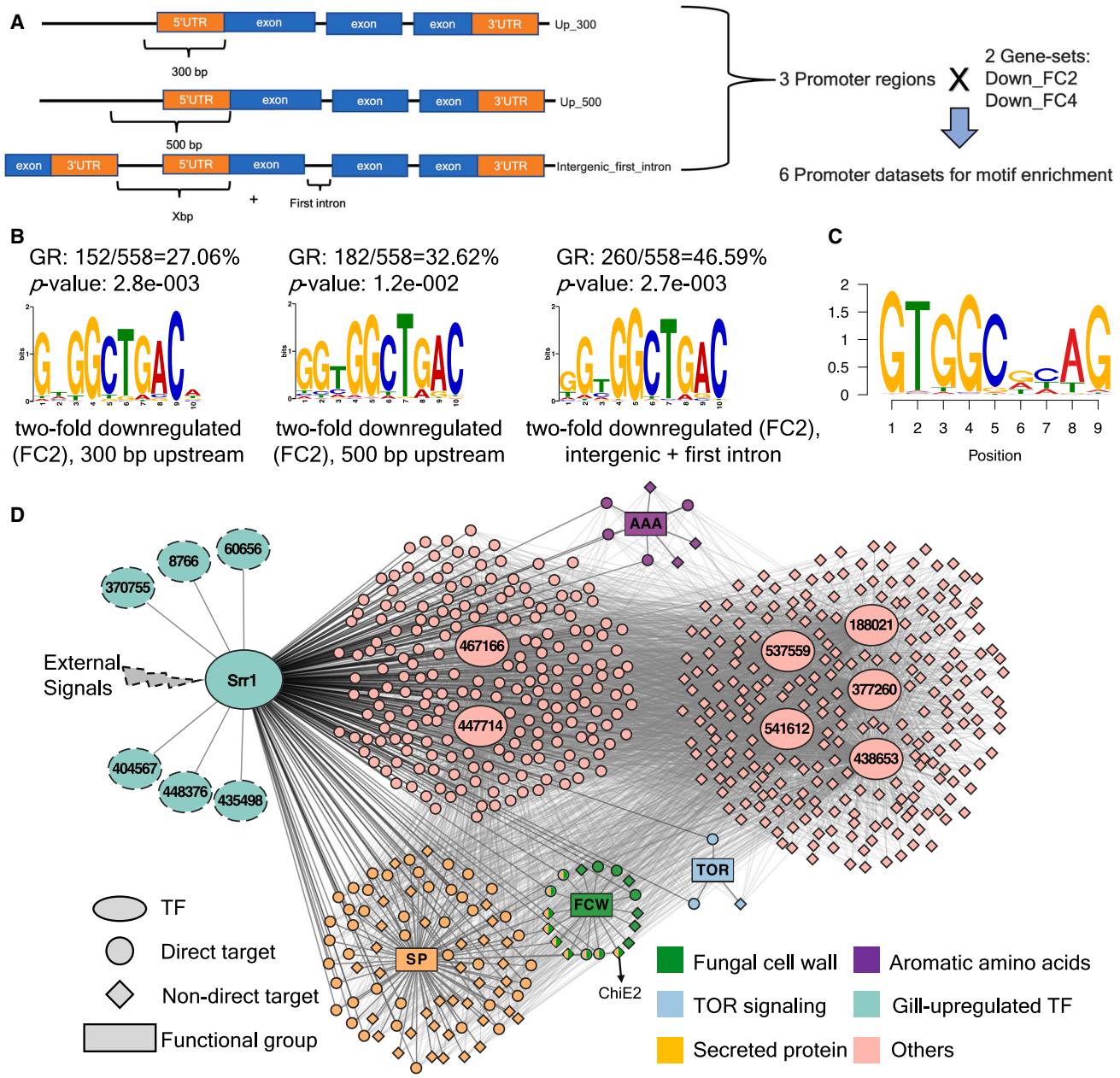

Figure 5. Motif analysis downregulated DEGs and hypothetical gene regulatory network of Srr1

(A) Outline of the construction of six promoter datasets.

(B) Motifs inferred using the different promoter datasets of downregulated genes (FC2). GR, gene ratio, refers to the ratio of genes with the motif occurring in its promoter, relative to all downregulated genes tested; *p* value refers to the binomial test result for the enrichment.

(C) Binding motif of Srr1 inferred using a sequence-based binding site predictor (https://zf.princeton.edu).

(D) Hypothetical gene regulatory network of Srr1. Shapes and colors represent gene/protein type and functional groups, respectively. Dashed lines connecting upstream transcription factors to Srr1 are hypothesized solely based on their tissue-specific expression patterns.

See also Figure S5 and Data S3.

correlate with that of ballistospory and overlap with Δ*srr1* downregulated DEGs. Global phylostratigraphy of Δ*srr1*-downregulated DEGs indicated that they originated mostly in the Basidiomycota, which differs considerably from the genome-wide phylostratigraphic pattern of most genes being ancient or very young.[29] This is consistent with ballistospore formation being a basidiomycete innovation. At the same time, we did not detect an enrichment of gene origins at the crown node of the Basidiomycota, where ballistospory has conceivably emerged in evolution (Figure 6A). Therefore, we focused on genes that show correlated losses with ballistospory, that is, mostly absent in independent lineages of secondarily non-ballistospotic species.

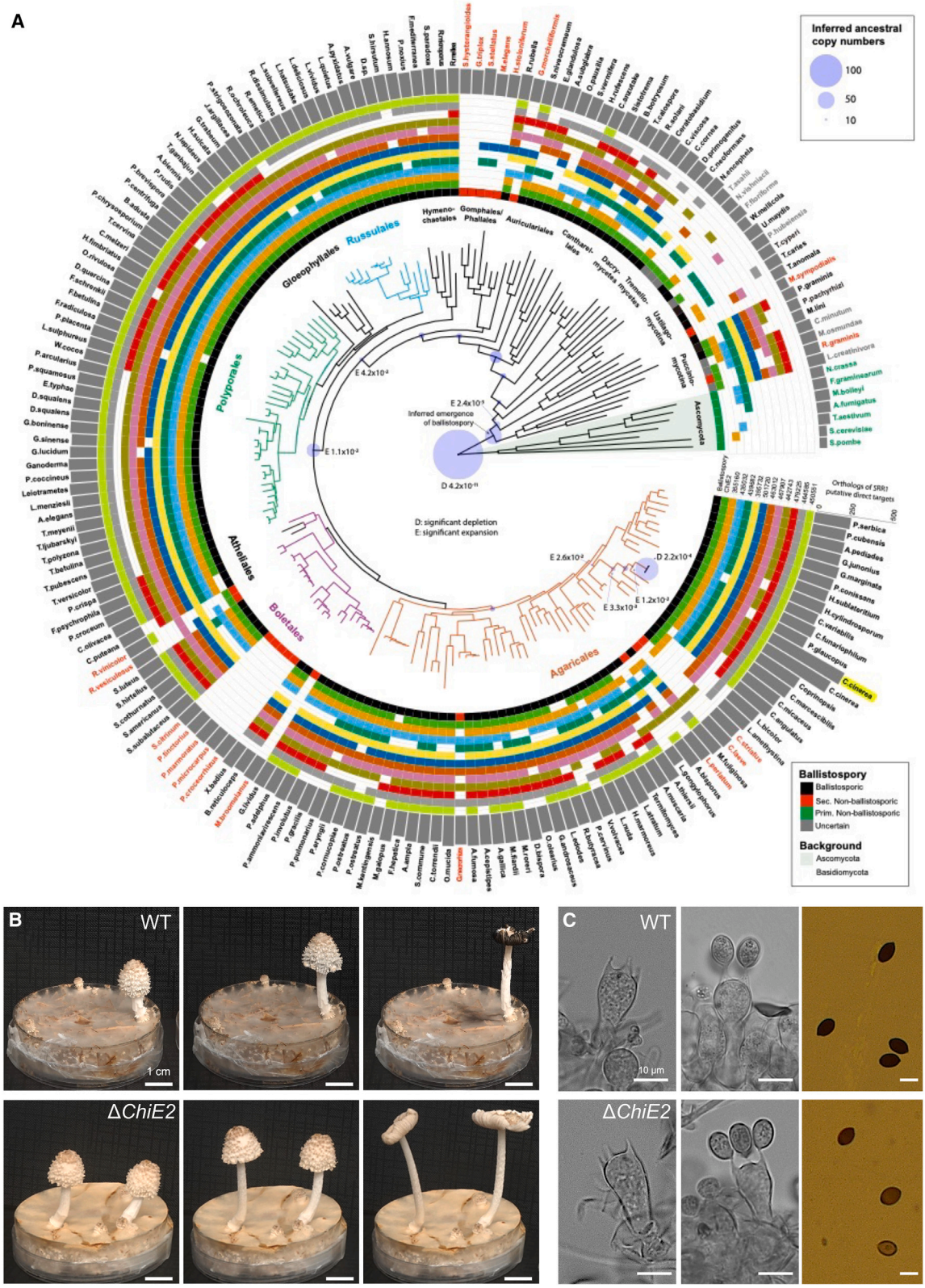

(legend on next page)

We hypothesized that genes linked to ballistospory may have been lost in some or all of the eight secondarily non-ballistosporic lineages (Figure 6A). We searched for genes conserved in >50% of ballistosporic species, lost in at least five secondarily non-ballistosporic lineages, and that show conserved lamellae-specific expression based on previous studies.[28,40] Using this strategy, we identified 12 orthogroups (Figure 6A; Data S5), which encode two cell-wall-related proteins, a nucleotide-sugar transferase, a peptidase, a serine-threonine exporter, and a GH25 lysozyme, among others. Two genes related to the fungal cell wall included a putative expansin (467907) and the GH18 family chitinase ChiE2 (520359), which was downregulated in the Δ*srr1* strain. This gene and its orthologs showed the highest expression in the lamellae of *C. cinerea*, *Armillaria ostoyae*, *Lentinus tigrinus*, and *P. ostreatus* and caps of *L. bicolor* and *Lentinula edodes* (separate lamellae samples were not available in these two species), consistent with a narrow role in sporulation.[40] Phylogenetic analyses of ChiE2 orthologs and related chitinases confirmed the phylostratigraphic and gene loss patterns for this gene (Figure S6).

To test whether *ChiE2* is involved in ballistospory, we generated deletion mutants in *C. cinerea*. The Δ*ChiE2* strains showed normal fruiting body development, including proper autolysis, and normal basidia with curved sterigmata but produced spore-poor caps compared with the WT (Figures 6B, S7D, and S7E; Video S2). The Δ*ChiE2* strain produced asymmetrical spores that had a lighter color and less-consistent shape than those of WT (Figure 6C), suggesting spore inflation, maturation, or shape problems. In line with macroscopic observations, Δ*ChiE2* had a significantly lower number of basidiospores than the WT (Figure S7E). The length and aspect ratio of the spores were also different and more variable in the Δ*ChiE2* strain than in the WT strain (Figure S7E). Because autolysis and powered spore discharge happen simultaneously in *C. cinerea*, observing the latter and testing whether the *ChiE2* knockout affected ballistospory directly is challenging. Nevertheless, spore asymmetry, a prerequisite of ballistospory, was observed in the mutant,[5,41] although spore shape, size and aspect ratio showed large variability, which might affect spore discharge. Considering all above, the results suggest that *ChiE2* is a sporulation-specific chitinase that perhaps participates in spore wall assembly/remodeling to ensure proper spore shaping, a prerequisite for ballistospory.

DISCUSSION

One of the most fundamental events in fungal development is spore production. Although the mechanisms and some genes involved in sporulation have been characterized in Ascomycota,[42–45] the genetics of sporulation remains poorly understood in Basidiomycota. In this study, we systematically addressed the genetics of spore formation for the first time in a model basidiomycete fungus, *C. cinerea*. We described a novel transcriptional regulator (*srr1*) and transcriptional events associated with post-meiotic events of sporulation. We inferred a broad but specific set of functions required for spore formation and a putative gene network downstream of Srr1, which includes direct and indirect regulatory links. Based on the *srr1* RNA-seq data, comparative genomics, and phylostratigraphy, we attempted to identify genes linked to ballistospory.

Srr1 is a TF in the C2H2 family and is conserved across the Agaricomycetes. The *srr1* knockout mutant produced healthy fruiting bodies without spores due to a postmeiotic arrest of sporogenesis after the emergence of spore initials at sterigmata tips. This phenotype corresponds to what has previously been reported as white cap or sporeless mutants in *C. cinerea*.[16,46,47] Among these, the *srr1* phenotype belong to the group that aborts development at prespore formation, in which at least 13 genes have been reported but not identified using ultraviolet mutagenesis,[46] and srr1 might be one of them. Most such mutations affect meiotic or DNA-repair genes (reviewed in Kües[7]), whereas Srr1 affects the postmeiotic process, which opened the way for dissecting morphogenetic aspects of sporulation. Understanding spore morphogenesis is of great importance in industry. Sporeless mutants are in great demand in crop and other mushroom production as they alleviate problems caused by spore production.[25,27,48,49] We anticipate that *srr1* or its target genes could be targets of breeding novel sporeless strains of commercially cultivated species, such as *Pleurotus* spp. or *Lentinula edodes*.

To identify the postmeiotic genetic toolkit of *C. cinerea*, we identified genes downstream of Srr1 using RNA-seq on the deletion mutant. Genes that failed to be activated in the mutant compared with the WT included ones related to the fungal cell wall, AAA biosynthesis, TOR signaling, and secreted proteins, among others. The promoters of the 559 downregulated genes provided a sharp signal for a binding motif of Srr1, which is supported by an independent, protein-sequence-based predictor. This allowed the inference of putative Srr1 target genes, even in the absence of ChIP-seq, which has not yet been successfully used in *C. cinerea*. Phylostratigraphy indicated that some of these genes are specific to *C. cinerea* (Figure 6A); however, the majority of genes are conserved, allowing us to make inferences on conserved mechanisms underlying spore formation in the Agaricomycetes.

Figure 6. Phylostratigraphic analysis for putative Srr1 target genes, candidate genes related to ballistospory, and phenotype comparison of Δ*ChiE2* and wild type

(A, D, and E) Phylostratigraphic analysis for Srr1 target genes and candidate genes related to ballistospory. The species tree depicts the 189 species used in the analyses. The occurrence of ballistospory and its absence in secondarily non-ballistosporic species (20 species in eight independent lineages in our dataset) are shown by the innermost track with black and red, respectively. Phylostratigraphic analysis of downregulated DEGs in the Δsrr1 strain (blue bubbles) illustrates the enrichment of gene origins in Basidiomycota nodes, circle size proportional to gene numbers. Numbers next to the node show significant *p* values (FET) with enrichment (E) or depletion (D). Twelve candidate ballistospory-related genes are shown by colored tracks (white means missing); these are mostly absent in non-ballistosporic lineages but conserved among other Basidiomycota. Gray bars show the number of orthologs of Srr1 DEGs present in each species. Complete species names can be found in Data S4.

(B) Fruiting bodies during developmental stages preceding sporulation of Δ*ChiE2* and WT.

(C) Basidial morphology and spores of Δ*ChiE2* and WT.

See also Figures S6 and S7 and Data S4 and S5 and Video S2.

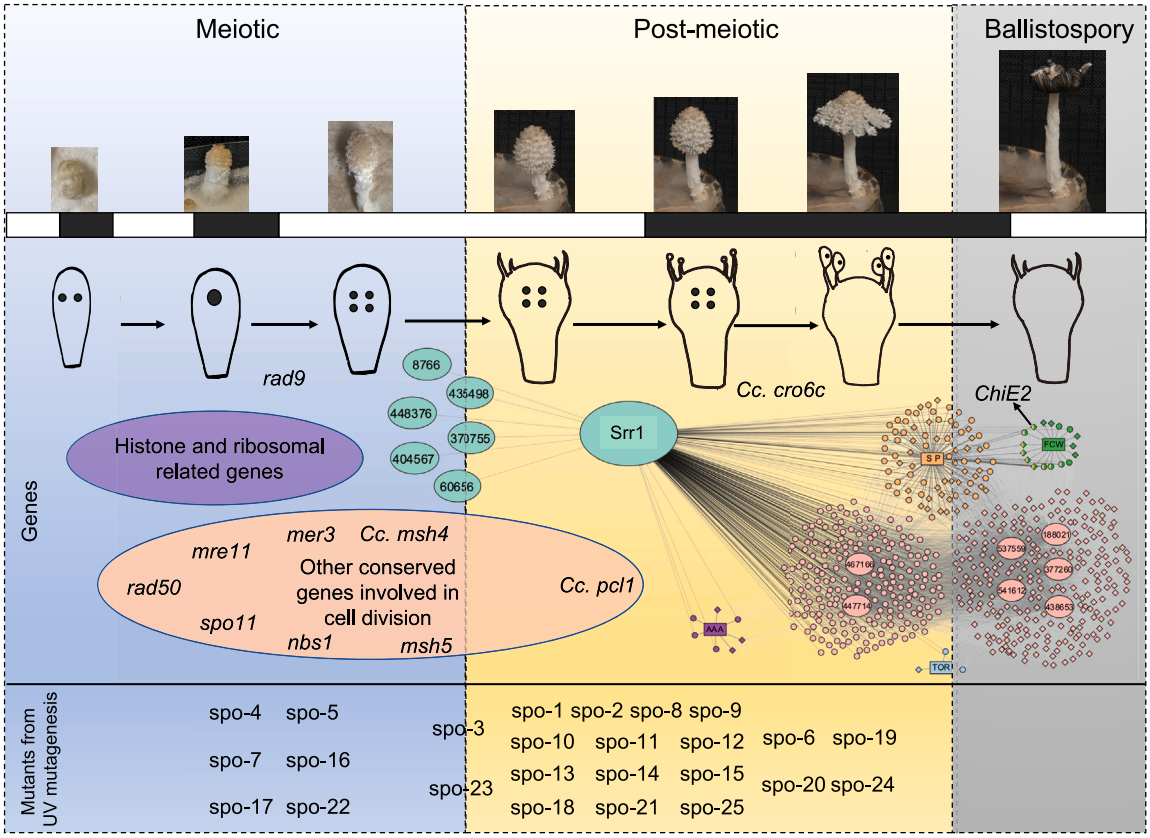

Figure 7. A synthesis on the genetics of sporulation based on this and previous studies

The black/white bars represent the ~12-h dark/light period (not to scale). Characterized genes (upper row) and mutants (lower row) are arranged according to their literature-reported arrest points. The purple ellipse represents the histone and ribosomal-protein-encoding genes,[40] the orange ellipse represents the ~180 conserved genes involved in cell division, including the characterized genes *mer3*,[15] *msh5*,[50] *rad50*,[51] *nbs1*,[52] *mre11*,[53] *spo11*,[54] *Cc. msh4* (*C. cinerea* ortholog of *msh4* in *P. pulmonarius*[26] and *P. ostreatus*[25]), and *Cc. pcl1* (*C. cinerea* ortholog of *pcl1* in *P. ostreatus*[55]). The listed UV mutagenesis mutants are from Kanda et al.[46] The hypothetical gene regulatory network is rearranged from Figure 5D, which is proposed in this study.

These data enabled a synthesis on the genetics of sporulation in mushroom-forming fungi. Figure 7 combines information from mutant analyses[46,50–52] and transcriptomic, genomic,[40] and reverse genetics studies,[15,25,26,53–55] as well as the Srr1 data, and complements the morphological description of sporulation available from prior literature.[7] Spore formation can be divided into three main stages, meiotic, postmeiotic/morphogenetic, and spore discharge. During the meiotic phase, karyogamy, meiosis and postmeiotic mitosis are associated with higher transcript levels of genes related to DNA replication, repair, chromosome positioning, cell-cycle regulation, and other related processes.[40] Several of these have been identified through mutant analyses, such as *mer3*,[15] *msh5*,[50] *rad50*,[51] *nbs1*,[52] *mre11*,[53] and *spo11*,[54] which are included in a core set of ~180 conserved genes involved in meiosis/mitosis that we circumscribed recently.[40] These also include the *C. cinerea* ortholog of *pcl1* described recently[55] and the *C. cinerea* ortholog of *msh4*, which is the gene mutated in existing sporeless oyster mushroom strains.[25,26] Concomitantly, histone and ribosomal-protein-encoding genes are upregulated, perhaps to support chromatin remodeling and protein production before spore formation.[40] The meiotic phase includes at least six TFs upstream of Srr1 that may link the meiotic phase with spore morphogenesis. It perhaps also includes cell-cycle regulators, which provide checkpoints between phases, although these are currently unknown. Srr1 may be a main regulator of the postmeiotic events (e.g., spore morphogenesis), regulating, according to our inferences, at least 260 genes directly and another ~300 indirectly. These include diverse functions as well as seven further TFs (see Figure 5D). The function of individual genes in this phase is poorly understood and characterizations remain to be done in future studies. The final, ballistospory stage, which includes the active discharge of spores from basidia, is genetically also poorly understood. It may include genes downstream of Srr1; however, there is little data on their identity.

Ballistospory is one of the defining traits of the Basidiomycota. We reasoned that, as spore formation is a penultimate event in mushroom development, genes linked to ballistospory should be downstream of Srr1 and that they should be missing in secondarily non-ballistosporic Agaricomycetes (e.g., puffballs and false truffles). Using phylostratigraphy and comparative genomics, we identified 12 candidate genes, including a downregulated GH18 chitinase (*ChiE2*), in the *srr1* mutant. Goughenour et al. showed that ChiE2 (ID: Copci1_341 in the reference) belongs to the A-III-type chitinase, which is highly reduced in Ascomycota and absent in the non-ballistosporic Basidiomycota

order Malasseziales.[56] Deletion of *ChiE2* in *C. cinerea* results in abnormal spore shape, with a partial loss of asymmetry but healthy fruiting bodies, which suggests that ChiE2 has sporulation-specific functions in basidiomycetes. As spore symmetry is an important feature of actively discharged basidiospores and ChiE2 orthologs are lost in secondarily non-ballistosporic species, we speculate it may be involved in this process. However, it is also plausible that secondarily non-ballistosporic taxa lost ChiE2 for reasons other than forcible spore discharge. In addition to *ChiE2*, further genes are certainly required for ballistospory, which remain to be identified in future studies. Nevertheless, our analyses provided the first genetic insights into this unique process and we anticipate that future analyses of Srr1 target genes will reveal further genes involved.

Taken together, this study has provided novel insights into the genetics of postmeiotic spore morphogenesis, one of the fundamental events in the life cycle of basidiomycetes. Although the genetics of these processes is certainly more complex than what this study could decipher, we anticipate that our results will contribute to understanding the general principles of sexual spore dispersal in a large and diverse group of fungi and will inspire further research on spore morphogenesis and mushroom biotechnology.

RESOURCE AVAILABILITY

Lead contact

Requests for further information and resources should be directed to and will be fulfilled by the lead contact, László G. Nagy (lnagy@fungenomelab.com).

Materials availability

Plasmids and mutant strains generated for this study are available upon request.

Data and code availability

- The collection of transcriptome raw data has been deposited at the NCBI's Gene Expression Omnibus (GEO) under the accession number GEO: GSE269820 and is publicly available as of the date of publication.
- The original code generated for data analysis is available on GitHub (https://github.com/Zhihao66/Srr1).
- Any additional information required to reanalyze the data reported in this paper is available from the lead contact upon request.

ACKNOWLEDGMENTS

We acknowledge support by the "Momentum" program of the Hungarian Academy of Sciences (contract no. LP2019-13/2019 to L.G.N.), the National Research Development and Innovation Office (grant no. OTKA 142188), the European Research Council (grant no. 101086900 to L.G.N.), the Eötvös Loránd Research Network (SA-109/2021, to L.G.N.), and the National Key Research and Development Program of China (2022YFD1200600, to W.G.). Z.H. acknowledges the support of China Scholarship Council (grant no. 202008110168) and Stipendium Hungaricum Scholarship (grant nos. SHE-21070-006/2020 and SHE-21070-009/2020). Z.M. was supported by the Janos Bolyai Research Scholarship of the Hungarian Academy of Sciences (BO/00269/24/8).

AUTHOR CONTRIBUTIONS

Z.H. and L.G.N. conceived the study. Z.H., Y.Y., Y.Z., A.C., C.F., H.W., Z.K., E.A., N.M., M.V., X.-B.L., Z.L., N.Z., and I.K. performed the wet-lab experiments. Z.H., Z.M., B.B., and B.H. processed the bioinformatics data. Z.H., Z.M., Y.Y., L.G.N., and W.G. analyzed the data and prepared figures. Z.H., L.G.N., Z.M., and W.G. wrote the original manuscript. All authors have read and commented on the manuscript.

DECLARATION OF INTERESTS

The authors declare no competing interests.

STAR★METHODS

Detailed methods are provided in the online version of this paper and include the following:

- KEY RESOURCES TABLE
- EXPERIMENTAL MODEL AND STUDY PARTICIPANT DETAILS
  - Gene expression datasets
  - Strains and culture media
- METHOD DETAILS
  - Plasmid construction, transformation, RNA interference and the mutant screening
  - Phenotyping of *C. cinerea*
  - Phenotyping of *P. cornucopiae*
  - RNA-sequencing and data analysis
  - Motif analyses and construction of a regulatory network
  - Phylogenetic and phylostratigraphic analyses
- QUANTIFICATION AND STATISTICAL ANALYSIS

SUPPLEMENTAL INFORMATION

Supplemental information can be found online at https://doi.org/10.1016/j.cub.2025.02.025.

Received: December 5, 2024
Revised: February 6, 2025
Accepted: February 13, 2025
Published: March 17, 2025

REFERENCES

1. Kadowaki, K., Leschen, R.A., and Beggs, J.R. (2010). Periodicity of spore release from individual Ganoderma fruiting bodies in a natural forest. Australas. Mycol. *29*, 17–23.
2. Dressaire, E., Yamada, L., Song, B., and Roper, M. (2016). Mushrooms use convectively created airflows to disperse their spores. Proc. Natl. Acad. Sci. USA *113*, 2833–2838. https://doi.org/10.1073/pnas.1509612113.
3. Anees-Hill, S., Douglas, P., Pashley, C.H., Hansell, A., and Marczylo, E.L. (2022). A systematic review of outdoor airborne fungal spore seasonality across Europe and the implications for health. Sci. Total Environ. *818*, 151716. https://doi.org/10.1016/j.scitotenv.2021.151716.
4. Hassett, M.O., Fischer, M.W.F., and Money, N.P. (2015). Mushrooms as Rainmakers: How Spores Act as Nuclei for Raindrops. PLoS One *10*, e0140407. https://doi.org/10.1371/journal.pone.0140407.
5. Money, N.P. (2023). Goldilocks mushrooms: How ballistospory has shaped basidiomycete evolution. Fungal Biol. *127*, 975–984. https://doi.org/10.1016/j.funbio.2023.02.004.
6. McLaughlin, D.J. (1977). Basidiospore Initiation and Early Development in Coprinus cinereus. Am. J. Bot. *64*, 1–16. https://doi.org/10.2307/2441870.
7. Kües, U. (2000). Life history and developmental processes in the basidiomycete Coprinus cinereus. Microbiol. Mol. Biol. Rev. *64*, 316–353. https://doi.org/10.1128/MMBR.64.2.316-353.2000.
8. Yoon, K.S., and McLaughlin, D.J. (1986). Basidiosporogenesis in Boletus rubinellus II. Late Spore Development. Mycologia *78*, 185–197. https://doi.org/10.2307/3793163.

9. Yoon, K.S., and McLaughlin, D.J. (1980). Fluorescence Microscopic Examination of Basidiosporogenesis in Boletus rubinellus and Coprinus cinereus. Mycologia *72*, 1150–1158. https://doi.org/10.2307/3759569.

10. Burge, H.A. (1979). Basidiospore Structure and Development in the Genus Russula. Mycologia *71*, 977–995. https://doi.org/10.2307/3759286.

11. Pringle, A., Patek, S.N., Fischer, M., Stolze, J., and Money, N.P. (2005). The Captured Launch of a Ballistospore. Mycologia *97*, 866–871.

12. Money, N.P. (2023). The fastest short jump in nature: Progress in understanding the mechanism of ballistospore discharge. Fungal Biol. *127*, 835–844. https://doi.org/10.1016/j.funbio.2023.01.001.

13. Iapichino, M., Wang, Y.W., Gentry, S., Pringle, A., and Seminara, A. (2021). A precise relationship among Buller's drop, ballistospore, and gill morphologies enables maximum packing of spores within gilled mushrooms. Mycologia *113*, 300–311. https://doi.org/10.1080/00275514.2020.1823175.

14. Fischer, M.W.F., Stolze-Rybczynski, J.L., Cui, Y., and Money, N.P. (2010). How far and how fast can mushroom spores fly? Physical limits on ballistospore size and discharge distance in the Basidiomycota. Fungal Biol. *114*, 669–675. https://doi.org/10.1016/j.funbio.2010.06.002.

15. Sugawara, H., Iwabata, K., Koshiyama, A., Yanai, T., Daikuhara, Y., Namekawa, S.H., Hamada, F.N., and Sakaguchi, K. (2009). Coprinus cinereus Mer3 is required for synaptonemal complex formation during meiosis. Chromosoma *118*, 127–139. https://doi.org/10.1007/s00412-008-0185-1.

16. Cummings, W.J., Celerin, M., Crodian, J., Brunick, L.K., and Zolan, M.E. (1999). Insertional mutagenesis in Coprinus cinereus: use of a dominant selectable marker to generate tagged, sporulation-defective mutants. Curr. Genet. *36*, 371–382. https://doi.org/10.1007/s002940050512.

17. Mikosch, T.S.P., Sonnenberg, A.S.M., and Van Griensven, L.J.L.D. (2002). Isolation, characterisation and expression patterns of a RAD51 ortholog from Pleuotus ostreatus. Mycol. Res. *106*, 682–687. https://doi.org/10.1017/S0953756202005877.

18. Pukkila, P.J. (1996). Production and Analysis of Meiotic Mutants in Coprinus cinereus. In Fungal Genetics: Principles and Practice, *363* (CRC Press).

19. Pukkila, P.J., and Casselton, L.A. (1991). Molecular genetics of the agaric Coprinus cinereus. In More Gene Manipulations in Fungi (Elsevier), pp. 126–150.

20. Pukkila, P.J., and Lu, B.C. (1985). Silver staining of meiotic chromosomes in the fungus, Coprinus cinereus. Chromosoma *91*, 108–112. https://doi.org/10.1007/BF00294053.

21. Mikosch, T.S., Sonnenberg, A.S., and Van Griensven, L.J. (2001). Isolation, characterization, and expression patterns of a DMC1 homolog from the basidiomycete Pleurotus ostreatus. Fungal Genet. Biol. *33*, 59–66. https://doi.org/10.1006/fgbi.2001.1265.

22. Baars, J., Sonnenberg, A.S., Mikosch, T., and Van Griensven, L. (2000). Development of a sporeless strain of oyster mushroom Pleurotus ostreatus. In Science and Cultivation of Edible Fungi. Proceedings of the 15th International Congress on the Science and Cultivation of Edible Fungi, L.J.L.D. van Griensven, ed., pp. 317–323.

23. Barh, A., Sharma, V.P., Annepu, S.K., Kamal, S., Sharma, S., and Bhatt, P. (2019). Genetic improvement in Pleurotus (oyster mushroom): a review. 3 Biotech *9*, 322. https://doi.org/10.1007/s13205-019-1854-x.

24. Yamasaki, F., Nakazawa, T., Sakamoto, M., and Honda, Y. (2021). Molecular breeding of sporeless strains of Pleurotus ostreatus using a non-homologous DNA end-joining defective strain. Mycol. Prog. *20*, 73–81. https://doi.org/10.1007/s11557-020-01661-w.

25. Lavrijssen, B., Baars, J.P., Lugones, L.G., Scholtmeijer, K., Sedaghat Telgerd, N., Sonnenberg, A.S.M., and van Peer, A.F. (2020). Interruption of an MSH4 homolog blocks meiosis in metaphase I and eliminates spore formation in Pleurotus ostreatus. PLoS One *15*, e0241749. https://doi.org/10.1371/journal.pone.0241749.

26. Okuda, Y., Murakami, S., Honda, Y., and Matsumoto, T. (2013). An MSH4 homolog, stpp1, from Pleurotus pulmonarius is a "silver bullet" for resolving problems caused by spores in cultivated mushrooms. Appl. Environ. Microbiol. *79*, 4520–4527. https://doi.org/10.1128/AEM.00561-13.

27. Obatake, Y., Murakami, S., Matsumoto, T., and Fukumasa-Nakai, Y. (2003). Isolation and characterization of a sporeless mutant in Pleurotus eryngii. Mycoscience *44*, 33–40. https://doi.org/10.1007/S10267-002-0074-Z.

28. Krizsán, K., Almási, É., Merényi, Z., Sahu, N., Virágh, M., Kószó, T., Mondo, S., Kiss, B., Bálint, B., Kües, U., et al. (2019). Transcriptomic atlas of mushroom development reveals conserved genes behind complex multicellularity in fungi. Proc. Natl. Acad. Sci. USA *116*, 7409–7418. https://doi.org/10.1073/pnas.1817822116.

29. Merényi, Z., Virágh, M., Gluck-Thaler, E., Slot, J.C., Kiss, B., Varga, T., Geösel, A., Hegedüs, B., Bálint, B., and Nagy, L.G. (2022). Gene age shapes the transcriptional landscape of sexual morphogenesis in mushroom-forming fungi (Agaricomycetes). eLife *11*, e71348. https://doi.org/10.7554/eLife.71348.

30. Ruytinx, J., Miyauchi, S., Hartmann-Wittulsky, S., de Freitas Pereira, M., Guinet, F., Churin, J.L., Put, C., Le Tacon, F., Veneault-Fourrey, C., Martin, F., and Kohler, A. (2021). A Transcriptomic Atlas of the Ectomycorrhizal Fungus Laccaria bicolor. Microorganisms *9*, 2612. https://doi.org/10.3390/microorganisms9122612.

31. Orban, A., Weber, A., Herzog, R., Hennicke, F., and Rühl, M. (2021). Transcriptome of different fruiting stages in the cultivated mushroom Cyclocybe aegerita suggests a complex regulation of fruiting and reveals enzymes putatively involved in fungal oxylipin biosynthesis. BMC Genomics *22*, 324. https://doi.org/10.1186/s12864-021-07648-5.

32. Pareek, M., Hegedüs, B., Hou, Z., Csernetics, Á., Wu, H., Virágh, M., Sahu, N., Liu, X.B., and Nagy, L. (2022). Preassembled Cas9 Ribonucleoprotein-Mediated Gene Deletion Identifies the Carbon Catabolite Repressor and Its Target Genes in Coprinopsis cinerea. Appl. Environ. Microbiol. *88*, e0094022. https://doi.org/10.1128/aem.00940-22.

33. Carrillo, A.J., Schacht, P., Cabrera, I.E., Blahut, J., Prudhomme, L., Dietrich, S., Bekman, T., Mei, J., Carrera, C., Chen, V., et al. (2017). Functional Profiling of Transcription Factor Genes in Neurospora crassa. G3 (Bethesda) *7*, 2945–2956. https://doi.org/10.1534/g3.117.043331.

34. McLaughlin, D.J. (1982). Ultrastructure and Cytochemistry of Basidial and Basidiospore Development. In Basidium and Basidiocarp: Evolution, Cytology, Function, and Development, K. Wells, and E.K. Wells, eds. (Springer), pp. 37–74. https://doi.org/10.1007/978-1-4612-5677-9_3.

35. Hegedüs, B., Sahu, N., Bálint, B., Haridas, S., Bense, V., Merényi, Z., Virágh, M., Wu, H., Liu, X.-B., Riley, R., et al. (2024). Unraveling Morphogenesis, Starvation, and Light Responses in a Mushroom-Forming Fungus, Coprinopsis cinerea, Using Long Read Sequencing and Extensive Expression Profiling. Preprint at bioRxiv. https://doi.org/10.1101/2024.05.10.593147.

36. Nosanchuk, J.D., Stark, R.E., and Casadevall, A. (2015). Fungal Melanin: What do We Know About Structure? Front. Microbiol. *6*, 1463. https://doi.org/10.3389/fmicb.2015.01463.

37. Baker, K., Kirkham, S., Halova, L., Atkin, J., Franz-Wachtel, M., Cobley, D., Krug, K., Maček, B., Mulvihill, D.P., and Petersen, J. (2016). TOR complex 2 localises to the cytokinetic actomyosin ring and controls the fidelity of cytokinesis. J. Cell Sci. *129*, 2613–2624. https://doi.org/10.1242/jcs.190124.

38. Myburgh, M.W., Schwerdtfeger, K.S., Cripwell, R.A., van Zyl, W.H., and Viljoen-Bloom, M. (2023). Promoters and introns as key drivers for enhanced gene expression in Saccharomyces cerevisiae. Adv. Appl. Microbiol. *124*, 1–29. https://doi.org/10.1016/bs.aambs.2023.07.002.

39. Persikov, A.V., and Singh, M. (2014). De novo prediction of DNA-binding specificities for Cys2His2 zinc finger proteins. Nucleic Acids Res. *42*, 97–108. https://doi.org/10.1093/nar/gkt890.

40. Nagy, L.G., Vonk, P.J., Künzler, M., Földi, C., Virágh, M., Ohm, R.A., Hennicke, F., Bálint, B., Csernetics, Á., Hegedüs, B., et al. (2023). Lessons on fruiting body morphogenesis from genomes and transcriptomes of Agaricomycetes. Stud. Mycol. *104*, 1–85. https://doi.org/10.3114/sim.2022.104.01.

41. Wilson, A.W., Binder, M., and Hibbett, D.S. (2011). Effects of gasteroid fruiting body morphology on diversification rates in three independent clades of fungi estimated using binary state speciation and extinction analysis. Evolution *65*, 1305–1322. https://doi.org/10.1111/j.1558-5646.2010.01214.x.

42. Cavinder, B., Sikhakolli, U., Fellows, K.M., and Trail, F. (2012). Sexual development and ascospore discharge in Fusarium graminearum. J. Vis. Exp. *61*, 3895. https://doi.org/10.3791/3895.

43. Min, K., Lee, J., Kim, J.C., Kim, S.G., Kim, Y.H., Vogel, S., Trail, F., and Lee, Y.W. (2010). A novel gene, ROA, is required for normal morphogenesis and discharge of ascospores in Gibberella zeae. Eukaryot. Cell *9*, 1495–1503. https://doi.org/10.1128/EC.00083-10.

44. Cavinder, B., Hamam, A., Lew, R.R., and Trail, F. (2011). Mid1, a mechanosensitive calcium ion channel, affects growth, development, and ascospore discharge in the filamentous fungus Gibberella zeae. Eukaryot. Cell *10*, 832–841. https://doi.org/10.1128/EC.00235-10.

45. Trail, F., and Seminara, A. (2014). The mechanism of ascus firing – Merging biophysical and mycological viewpoints. Fungal Biol. Rev. *28*, 70–76. https://doi.org/10.1016/j.fbr.2014.07.002.

46. Kanda, T., Goto, A., Sawa, K., Arakawa, H., Yasuda, Y., and Takemaru, T. (1989). Isolation and characterization of recessive sporeless mutants in the basidiomycete Coprinus cinereus. Mol. Gen. Genet. MGG *216*, 526–529. https://doi.org/10.1007/BF00334400.

47. Lu, B.C., Gallo, N., and Kües, U. (2003). White-cap mutants and meiotic apoptosis in the basidiomycete Coprinus cinereus. Fungal Genet. Biol. *39*, 82–93. https://doi.org/10.1016/s1087-1845(03)00024-0.

48. Yu, M., and Chang, S.T. (1989). Mutants ofPleurotus florida deficient in sporulation. World. J. Microbiol. Biotechnol. *5*, 487–492. https://doi.org/10.1007/BF01741824.

49. Hasebe, K., Murakami, S., and Tsuneda, A. (1991). Cytology and Genetics of a Sporeless Mutant of Lentinus Edodes. Mycologia *83*, 354–359. https://doi.org/10.2307/3759995.

50. Cummings, W.J., Merino, S.T., Young, K.G., Li, L., Johnson, C.W., Sierra, E.A., and Zolan, M.E. (2002). The Coprinus cinereus adherin Rad9 functions in Mre11-dependent DNA repair, meiotic sister-chromatid cohesion, and meiotic homolog pairing. Proc. Natl. Acad. Sci. USA *99*, 14958–14963. https://doi.org/10.1073/pnas.232316999.

51. Anderson, E., Burns, C., and Zolan, M.E. (2012). Global gene expression in Coprinopsis cinerea meiotic mutants reflects checkpoint arrest. G3 (Bethesda) *2*, 1213–1221. https://doi.org/10.1534/g3.112.003046.

52. Crown, K.N., Savytskyy, O.P., Malik, S.B., Logsdon, J., Williams, R.S., Tainer, J.A., and Zolan, M.E. (2013). A mutation in the FHA domain of Coprinus cinereus Nbs1 Leads to Spo11-independent meiotic recombination and chromosome segregation. G3 (Bethesda) *3*, 1927–1943. https://doi.org/10.1534/g3.113.007906.

53. Gerecke, E.E., and Zolan, M.E. (2000). An mre11 mutant of Coprinus cinereus has defects in meiotic chromosome pairing, condensation and synapsis. Genetics *154*, 1125–1139. https://doi.org/10.1093/genetics/154.3.1125.

54. Celerin, M., Merino, S.T., Stone, J.E., Menzie, A.M., and Zolan, M.E. (2000). Multiple roles of Spo11 in meiotic chromosome behavior. EMBO J. *19*, 2739–2750. https://doi.org/10.1093/emboj/19.11.2739.

55. Kobukata, T., Nakazawa, T., Yamasaki, F., Sugano, J., Oh, M., Kawauchi, M., Sakamoto, M., and Honda, Y. (2024). Identification of two genes essential for basidiospore formation during the postmeiotic stages in Pleurotus ostreatus. Fungal Genet. Biol. *172*, 103890. https://doi.org/10.1016/j.fgb.2024.103890.

56. Goughenour, K.D., Whalin, J., Slot, J.C., and Rappleye, C.A. (2021). Diversification of Fungal Chitinases and Their Functional Differentiation in Histoplasma capsulatum. Mol. Biol. Evol. *38*, 1339–1355. https://doi.org/10.1093/molbev/msaa293.

57. Andrews, S. (2010). FastQC: a quality control tool for high throughput sequence data (Cambridge). https://github.com/s-andrews/FastQC.

58. Bushnell, B., Rood, J., and Singer, E. (2017). BBMerge - Accurate paired shotgun read merging via overlap. PLoS One *12*, e0185056. https://doi.org/10.1371/journal.pone.0185056.

59. Dobin, A., Davis, C.A., Schlesinger, F., Drenkow, J., Zaleski, C., Jha, S., Batut, P., Chaisson, M., and Gingeras, T.R. (2013). STAR: ultrafast universal RNA-seq aligner. Bioinformatics *29*, 15–21. https://doi.org/10.1093/bioinformatics/bts635.

60. Liao, Y., Smyth, G.K., and Shi, W. (2014). featureCounts: an efficient general purpose program for assigning sequence reads to genomic features. Bioinformatics *30*, 923–930. https://doi.org/10.1093/bioinformatics/btt656.

61. Paysan-Lafosse, T., Blum, M., Chuguransky, S., Grego, T., Pinto, B.L., Salazar, G.A., Bileschi, M.L., Bork, P., Bridge, A., Colwell, L., et al. (2023). InterPro in 2022. Nucleic Acids Res. *51*, D418–D427. https://doi.org/10.1093/nar/gkac993.

62. Teufel, F., Almagro Armenteros, J.J., Johansen, A.R., Gíslason, M.H., Pihl, S.I., Tsirigos, K.D., Winther, O., Brunak, S., von Heijne, G., and Nielsen, H. (2022). SignalP 6.0 predicts all five types of signal peptides using protein language models. Nat. Biotechnol. *40*, 1023–1025. https://doi.org/10.1038/s41587-021-01156-3.

63. Steinegger, M., and Söding, J. (2017). MMseqs2 enables sensitive protein sequence searching for the analysis of massive data sets. Nat. Biotechnol. *35*, 1026–1028. https://doi.org/10.1038/nbt.3988.

64. Chen, C.J., Wu, Y., Li, J.W., Wang, X., Zeng, Z.H., Xu, J., Liu, Y.L., Feng, J.T., Chen, H., He, Y.H., and Xia, R. (2023). TBtools-II: A "one for all, all for one" bioinformatics platform for biological big-data mining. Mol. Plant *16*, 1733–1742. https://doi.org/10.1016/j.molp.2023.09.010.

65. Smoot, M.E., Ono, K., Ruscheinski, J., Wang, P.L., and Ideker, T. (2011). Cytoscape 2.8: new features for data integration and network visualization. Bioinformatics *27*, 431–432. https://doi.org/10.1093/bioinformatics/btq675.

66. Bailey, T.L. (2021). STREME: accurate and versatile sequence motif discovery. Bioinformatics *37*, 2834–2840. https://doi.org/10.1093/bioinformatics/btab203.

67. Löytynoja, A. (2014). Phylogeny-aware alignment with PRANK. Methods Mol. Biol. *1079*, 155–170. https://doi.org/10.1007/978-1-62703-646-7_10.

68. Capella-Gutiérrez, S., Silla-Martínez, J.M., and Gabaldón, T. (2009). trimAl: a tool for automated alignment trimming in large-scale phylogenetic analyses. Bioinformatics *25*, 1972–1973. https://doi.org/10.1093/bioinformatics/btp348.

69. Minh, B.Q., Schmidt, H.A., Chernomor, O., Schrempf, D., Woodhams, M.D., von Haeseler, A., and Lanfear, R. (2020). IQ-TREE 2: New Models and Efficient Methods for Phylogenetic Inference in the Genomic Era. Mol. Biol. Evol. *37*, 2461. https://doi.org/10.1093/molbev/msaa131.

70. Katoh, K., and Standley, D.M. (2013). MAFFT Multiple Sequence Alignment Software Version 7: Improvements in Performance and Usability. Mol. Biol. Evol. *30*, 772–780. https://doi.org/10.1093/molbev/mst010.

71. Stamatakis, A. (2014). RAxML version 8: a tool for phylogenetic analysis and post-analysis of large phylogenies. Bioinformatics *30*, 1312–1313. https://doi.org/10.1093/bioinformatics/btu033.

72. Wickham, H. (2009). ggplot2: Elegant Graphics for Data Analysis, H. Wickham, ed. (Springer), pp. 189–201. https://doi.org/10.1007/978-3-319-24277-4_9.

73. Schmieder, S.S., Stanley, C.E., Rzepiela, A., van Swaay, D., Sabotič, J., Nørrelykke, S.F., deMello, A.J., Aebi, M., and Künzler, M. (2019). Bidirectional Propagation of Signals and Nutrients in Fungal Networks via Specialized Hyphae. Curr. Biol. *29*, 217–228.e4. https://doi.org/10.1016/j.cub.2018.11.058.

74. Dörnte, B., Peng, C., Fang, Z., Kamran, A., Yulvizar, C., and Kües, U. (2020). Selection markers for transformation of the sequenced reference monokaryon Okayama 7/#130 and homokaryon AmutBmut of Coprinopsis cinerea. Fungal Biol. Biotechnol. *7*, 15. https://doi.org/10.1186/s40694-020-00105-0.

75. Xie, S.S., Shen, B., Zhang, C.B., Huang, X.X., and Zhang, Y.L. (2014). sgRNAcas9: A Software Package for Designing CRISPR sgRNA and Evaluating Potential Off-Target Cleavage Sites. PLoS One *9*, e100448. https://doi.org/10.1371/journal.pone.0100448.

76. Dörnte, B., and Kües, U. (2012). Reliability in transformation of the basidiomycete Coprinopsis cinerea. Curr. Trends Biotechnol. Pharm. *6*, 340–355.

77. Dornte, B., and Kües, U. (2013). Fast microwave-based DNA extraction from vegetative mycelium and fruiting body tissues of Agaricomycetes for PCR amplification. Curr. Trends Biotechnol. Pharm. *7*, 825–836.

78. Hou, L., Zhao, M., Huang, C., Wu, X., and Zhang, J. (2020). Nitric Oxide Improves the Tolerance of Pleurotus ostreatus to Heat Stress by Inhibiting Mitochondrial Aconitase. Appl. Environ. Microbiol. *86*, e0230319. https://doi.org/10.1128/AEM.02303-19.

79. Hou, L., Wang, L., Wu, X., Gao, W., Zhang, J., and Huang, C. (2019). Expression patterns of two pal genes of Pleurotus ostreatus across developmental stages and under heat stress. BMC Microbiol. *19*, 231. https://doi.org/10.1186/s12866-019-1594-4.

80. Constantin, A.-E., and Patil, I. (2021). ggsignif: R package for displaying significance brackets for 'ggplot2'. Preprint at PsyArxiv. https://doi.org/10.31234/osf.io/7awm6.

81. Love, M.I., Huber, W., and Anders, S. (2014). Moderated estimation of fold change and dispersion for RNA-seq data with DESeq2. Genome Biol. *15*, 550. https://doi.org/10.1186/s13059-014-0550-8.

82. Gu, Z. (2022). Complex heatmap visualization. Imeta *1*, e43. https://doi.org/10.1002/imt2.43.

83. McCarthy, D.J., Chen, Y., and Smyth, G.K. (2012). Differential expression analysis of multifactor RNA-Seq experiments with respect to biological variation. Nucleic Acids Res. *40*, 4288–4297. https://doi.org/10.1093/nar/gks042.

84. Blighe, K., Rana, S., and Lewis, M. (2021). EnhancedVolcano: Publication-ready volcano plots with enhanced colouring and labeling. https://bioconductor.org/packages/devel/bioc/vignettes/EnhancedVolcano/inst/doc/EnhancedVolcano.html.

85. Wu, T.Z., Hu, E.Q., Xu, S.B., Chen, M.J., Guo, P.F., Dai, Z.H., Feng, T.Z., Zhou, L., Tang, W.L., Zhan, L., et al. (2021). clusterProfiler 4.0: A universal enrichment tool for interpreting omics data. Innovation *2*, 100141. https://doi.org/10.1016/j.xinn.2021.100141.

86. Stajich, J.E., Wilke, S.K., Ahrén, D., Au, C.H., Birren, B.W., Borodovsky, M., Burns, C., Canbäck, B., Casselton, L.A., Cheng, C.K., et al. (2010). Insights into evolution of multicellular fungi from the assembled chromosomes of the mushroom Coprinopsis cinerea (Coprinus cinereus). Proc. Natl. Acad. Sci. USA *107*, 11889–11894. https://doi.org/10.1073/pnas.1003391107.

87. Wagih, O. (2017). ggseqlogo: a versatile R package for drawing sequence logos. Bioinformatics *33*, 3645–3647. https://doi.org/10.1093/bioinformatics/btx469.

88. Sonawane, A.R., Platig, J., Fagny, M., Chen, C.Y., Paulson, J.N., Lopes-Ramos, C.M., DeMeo, D.L., Quackenbush, J., Glass, K., and Kuijjer, M.L. (2017). Understanding Tissue-Specific Gene Regulation. Cell Rep. *21*, 1077–1088. https://doi.org/10.1016/j.celrep.2017.10.001.

89. R Core Team (2020). R: A language and environment for statistical computing (R Foundation for Statistical. Computing).

STAR★METHODS

KEY RESOURCES TABLE

REAGENT or RESOURCE	SOURCE	IDENTIFIER
Chemicals, peptides, and recombinant proteins		
Alt-R® CRISPR-Cas9 tracrRNA	Integrated DNA Technologies	Cat# 1072534
Alt-R™ S.p. Cas9 Nuclease V3	Integrated DNA Technologies	Cat# 10000735
Hoechst 33342	Thermo Fisher Scientific	Cat# H1399
Critical commercial assays		
Gibson Assembly Cloning Kit	NEB	Cat# E5510S
Quick-RNA Miniprep Kit	Zymo Research	Cat# R1055
HiScript Q RT SuperMix reverse transcription kit	Vazyme	Cat# R423
AceQ qPCR SYBR Green Master Mix	Vazyme	Cat# Q511
Deposited data		
RNA-Seq data of different developmental stages in *Coprinopsis cinerea*	Krizsán et al.[28]	GSE125184
RNA-Seq data of different developmental stages in *Pleurotus ostreatus*	Merényi et al.[29]	GSE176181
RNA-Seq data of different developmental stages in *Laccaria bicolor*	Ruytinx et al.[30]	GSE190443-GSE190445
RNA-Seq data of different developmental stages in *Cyclocybe aegerita*	Orban et al.[31]	PRJNA677924
RNA-Seq data of Δ*srr1* and wild type sample	This study	GSE269820
Experimental models: Organisms/strains		
Coprinopsis cinerea strain	Krizsán et al.[28]	A43mut B43mut pab1-1 #326
Pleurotus cornucopiae strain	China Centre for Mushroom Spawn Standards and Control	CCMSSC00406
Oligonucleotides		
Primers for plasmid construction and mutant screening	This study	Table S2
Recombinant DNA		
Plasmid: Srr1_KO_plasmid	This study	N/A
Plasmid: RNAi-g1654	This study	N/A
Plasmid: pUC19_PABA	This study	N/A
Software and algorithms		
FastQC (version 0.11.8)	Andrews et al.[57]	https://www.bioinformatics.babraham.ac.uk/projects/fastqc
bbduk.sh (version 38.92)	Bushnell et al.[58]	https://github.com/BioInfoTools/BBMap/blob/master/sh/bbduk.sh
STAR (version 2.6.1)	Dobin et al.[59]	https://github.com/alexdobin/STAR
Featurecount (version 2.0.1)	Liao et al.[60]	https://subread.sourceforge.net/
InterProScan (version 5.65-97.0)	Paysan-Lafosse et al.[61]	https://github.com/ebi-pf-team/interproscan
SignalP (version 6.0)	Teufel et al.[62]	https://dtu.biolib.com/SignalP-6
MMseqs2 (version 13.45111)	Steinegger et al.[63]	https://github.com/soedinglab/MMseqs2
TBtools (version 2.080)	Chen et al.[64]	https://github.com/CJ-Chen/TBtools-II
Cytoscape (version 3.10.2)	Smoot et al.[65]	https://cytoscape.org
Zinc finger protein prediction tool (last access 09/2023)	Persikov et al.[39]	https://zf.princeton.edu
STREME (version 5.5.7)	Bailey et al.[66]	https://meme-suite.org/meme/tools/streme
PRANK (version 170427)	Löytynoja et al.[67]	http://wasabiapp.org/software/prank/

(*Continued on next page*)

Continued

REAGENT or RESOURCE	SOURCE	IDENTIFIER
TrimAL (version 1.2rev59)	Capella-Gutiérrez et al.[68]	https://vicfero.github.io/trimal/
IQ-TREE (version 1.6.12)	Minh et al.[69]	http://www.iqtree.org/
Mafft (version 7)	Katoh et al.[70]	https://mafft.cbrc.jp/alignment/software/
RAxML (version 8.2.12)	Stamatakis et al.[71]	https://github.com/stamatak/standard-RAxML

EXPERIMENTAL MODEL AND STUDY PARTICIPANT DETAILS

Gene expression datasets

The raw RNA-Seq data of different developmental stages in *Coprinopsis cinerea* was obtained from Krizsán et al.,[28] and reanalysed using the reference genome and the reanalysis workflow by Hegedüs et al.[35] The raw expression data of *Pleurotus ostreatus*, *Laccaria bicolor* and *Cyclocybe aegerita* were obtained from the published developmental transcriptomes,[29–31] and the orthology relationships of Srr1 were generated from the results of Nagy et al.[40] Gene expression levels were shown in the line charts and expression fold-changes were shown with a barplot, plotted with the R package ggplot2.[72]

Strains and culture media

The homokaryotic *C. cinerea A43mut B43mut pab1-1* #326 strain and dikaryotic *P. cornucopiae* CCMSSC00406 strain (from China Centre for Mushroom Spawn Standards and Control) were used in this study. For oidiation of *C. cinerea*, small agar plugs were inoculated on yeast extract-malt extract-glucose (YMG) agar medium and cultured at 37 °C for 6-7 days under constant light to generate the oidia for the transformation. For fruiting *C. cinerea* on the Petri dish, the strains were grown on YMG (with 0.2% glucose) medium at 28 °C for 5-6 days until the mycelium reached ~1 cm of the edge of the Petri dish, then were transferred to white light for 2 h and back to dark for another 1 day, followed by a 12/12 h light/dark cycle for fruiting, at 28 °C with around 80% relative humidity. For phenotyping *C. cinerea* on straw, the substrate was prepared as follows: 75% straw and 25% wheat bran, with the water content around 80%. For *P. cornucopiae*, the Potato Dextrose Agar (PDA) medium was used for the basic culturing, and the substrate as follows was used for fruiting: 94% cottonseed hulls, 5% wheat bran, and 1% gypsum, with an approximate water content of 65%. Then polycarbonate plastic bottles (diameter=70 mm, height=90 mm, volume=280 ml) were filled with around 180 g of substrate and autoclaved for 2 hours at 0.11 MPa and 121 °C.

METHOD DETAILS

Plasmid construction, transformation, RNA interference and the mutant screening

For *C. cinerea*, the CRISPR/Cas9 system was used for gene deletion. The primers and crisprRNAs (crRNAs) are listed in Table S2. The backbone was linearized by the primer pair PUC19_F/PUC19_R for *srr1*, and by primer pair PUC19_F_1/PUC19_R_1 for *ChiE2* using pUC19 plasmid as a template. The native para-aminobenzoic acid (PABA) synthase gene (*pab1*) was amplified from the pMA412 vector using the primer pair Srr1_PABA_1F/Srr1_PABA_1R (for *srr1*) and primer pair PABA_F/PABA_R (for *ChiE2*) as the positive selection marker.[73,74] The upstream and downstream homology arms of *srr1* were amplified by the primer pairs Srr1_Up_1F/Srr1_Up_1R, and Srr1_Down_1F/Srr1_Down_1R, respectively, using genomic DNA as a template. The fragments were assembled by Gibson Assembly Cloning Kit (NEB, UK) according to the manufacturer's instructions. The assembled plasmid map is shown in Figure S2A for *srr1* and Figure S7A for *ChiE2*. Two sgRNAs (srr1_sgRNA_1 and srr1_sgRNA_2) were designed for *srr1* and one (ChiE2_sgRNA) for *ChiE2* by sgRNAcas9.[75] The *in vitro*-assembled RNP complexes were prepared using commercially synthesized trans-activating CRISPR RNA (tracrRNA) and CRISPR RNA (crRNA) according to the manufacturer's instructions (IDT, USA). For each *in vitro*-assembled RNP mixture, 1.2 μL of crRNA (100 μM), 1.2 μL of tracrRNA (100 μM) and 9.6 μL of duplex buffer were mixed. The duplexes were incubated at 95°C for 5 minutes, followed by cooling for 2 minutes. The RNA duplexes, along with Cas9 (10 μg/μL), 1.5 μL Cas9 working buffer, and 1.0 μL duplex buffer were then mixed and incubated at 37 °C for 15 minutes. Transformation of *C. cinerea* was conducted according to the protocol described by Dörnte et al.[76] and Pareek et al.[32] The DNA samples for screening transformants were prepared with the microwave-based method.[77] For *srr1*, the primer pair Srr1_Up_1F/Srr1_Down_1R was used for the first-round screening, samples with products in different sizes from WT (3906 bp) were selected for the second round of screening. The primer pair Srr1_GF/Srr1_GR was used for the second round of screening, and transformants with no WT band (1365 bp) were selected as clean mutants (Figures S2B–S2D). RT-PCR was also performed to verify the lack of transcription of srr1 using the primer pair Srr1_RT_1F/Srr1_RT_1R. For *ChiE2*, the primer pair ChiE2_CF/ChiE2_CR was used for PCR screening, because the plasmid can be multiple or partially integrated in the cleavage site, samples with missing (too long to amplify) or different sized (partially integrated) product from WT (845 bp) were selected as the mutants (Figures S7B–S7C).

For *P. cornucopiae*, the RNA interference (RNAi) method was conducted for the gene knockdown. The primers are listed in Table S2. An RNAi plasmid was constructed using the modified pCAMBIA1300 vector containing the hygromycin B phosphotransferase gene (*hyg*).[78] The RNAi-F and RNAi-R sequences were PCR amplified using genomic DNA from strain CCMSSC00406 as a

template and then ligated into the interference vector (Figure S3A). Subsequently, the RNAi plasmid was transferred into the wild-type strain using *Agrobacterium tumefaciens* GV3101, following previous research protocol.[79] Two rounds of selection of transformants were performed on complete yeast medium (CYM) supplemented with 90 mg/ml hygromycin B. Transformants with the highest interference efficiency were screened through quantitative PCR (qPCR) analysis. RNA extraction was performed using the E.Z.N.A. Plant RNA Kit (Omega Bio-Tek, Norcross, GA, USA), and cDNA was synthesised using the HiScript Q RT SuperMix reverse transcription kit (Vazyme, Nanjing, China). qPCR reactions were carried out using AceQ qPCR SYBR Green Master Mix (Vazyme, Nanjing, China) and an ABI 7500 real-time PCR amplifier (Applied Biosystems, Foster City, CA, USA). The amplification program included an initial denaturation at 95°C for 30 seconds, followed by 40 cycles of 95°C for 10 seconds, 60°C for 30 seconds, and extension at 72°C for 30 seconds. The $2^{-\Delta\Delta CT}$ method was used to calculate the relative gene expression levels, with the *β-actin* gene used as a reference.

Phenotyping of *C. cinerea*

For growth rate measurement, small agar plugs (d=5 mm) of wild-type and Δ*srr1* strains (3 replicates/group) were inoculated on the YMG (0.2% glucose) media and cultured at 28 °C in the dark. Colony diameters were measured every 24 h until 96 h. For testing the oidiation, wild-type and Δ*srr1* strains (3 replicates/group) were cultured on YMG (0.2% glucose) media at 37 °C under constant light for 4 days. The colony diameters were measured and the oidia were collected, counted and quantified by oidium number/mm^2. For analysis of fruiting body development, the strains were inoculated on the straw substrate and grown at 37 °C in the dark. After the mycelium was fully grown, they were transferred into the incubator with a 12/12 h light/dark cycle at 28 °C with ∼80% relative humidity for fruiting. Photos of fruiting bodies were taken in different developmental stages and the time-lapse videos were generated for monitoring the fruiting process. For basidiospore counting, the whole mature caps (after the fruiting body autolysis) were collected (7 for WT and 8 for Δ*ChiE2*), weighed and then were put into the 1.5ml Eppendorf tube with 500 μL water. The caps were smashed by the small pestle to detach the basidiospores. The basidiospores were counted and quantified by the number of spores/gram cap, the length and width of the spores (20 for each strain) were measured and the aspect ratio (length/width) was calculated. For data illustration, the line charts and the boxplots were plotted in R with the ggplot2 package,[72] and the Student's t-test was used to assign the significance with the ggsignif package.[80]

For checking the meiosis in Δ*srr1* and WT by microscopy, we took gill samples of WT and Δ*srr1* fruiting bodies when spore initials emerge at the sterigma tips (the Δ*srr1* arrest stage). Hoechst 33342 (0.1 μg/ml, Thermo Fisher Scientific, UK) was used for staining nuclei for 10 minutes, followed by 2 times washing using PBS buffer. The samples were checked under a fluorescence microscope both under bright and the blue channel. For comparing the morphology of basidia and basidiospores in WT and Δ*ChiE2*, we took the samples from the gill of the WT and Δ*ChiE2* fruiting bodies around the sterigmata formation and spore maturation stages (according to the definition of Kües[7]), and checked them under the optical microscope.

Phenotyping of *P. cornucopiae*

The *P. cornucopiae* strain was pre-cultured on the PDA media at 28 °C for 7 days in the dark. Well-grown agar plugs (3 pieces) were taken from PDA plates and inoculated into the substrate in the plastic bottles, followed by cultivation in the dark at 25 °C. After ∼15-20 days. The bottles were opened when the mycelium fully filled the substrate, then the surface-aged mycelium was removed, and the plastic bottles were transferred to environmental-controlled fruiting facilities at 18 °C. Relative air humidity was maintained at 85%-95%, light intensity was set at 300-500 lux with a daily illumination period of 12 hours, ventilation was performed 3-4 times, and CO_2 concentration was kept below 1000 ppm. Each experimental group included 20 replicates.

Spore quantification was conducted when the fruiting bodies reached maturity. Mature mushroom caps were carefully placed on glass slides, were let to drop spores, then covered with a coverslip, and observed under a microscope, with photographs taken. Mature mushroom caps were also placed on black paper, covered tightly, and after 12 hours, spore prints were obtained. A 0.5 x 0.5 cm portion was cut from the edge of the obtained spore print (where spores were most concentrated), rinsed thoroughly with 500 μL ddH_2O, resulting in a spore suspension. The suspension was then diluted tenfold, and spore counting was performed using a hemocytometer.

The formula for spore count per ml is given by:

Spore count (per ml) =Total number of spores in 80 small squares/(80×400×10000×10)

This calculation involves counting spores in 80 small squares, where each small square corresponds to a specific volume and dilution factor.

RNA-sequencing and data analysis

For collecting samples for the RNA-Seq, the gills were isolated by peeling cap and veil tissues off of gills using a scalpel and forceps from the Δ*srr1* and WT young fruiting bodies (3 replicates for each group) when spore initials emerge at the sterigma tips (Figure 4A), and put in the liquid nitrogen immediately. RNA extraction was performed using the Quick-RNA Miniprep Kit (Zymo Research, USA), non-strand-specific cDNA library and pair-end (150 bp) sequencing were conducted by Novogene Co., Ltd (Cambridge, UK) with a range of 41-54 million reads per sample. The raw reads were checked by FastQC (version 0.11.8),[57] and trimmed by bbduk.sh (version 38.92, qtrim=r trimq=10 minlength=20).[58] Trimmed reads were mapped to the reference genome using STAR (version 2.6.1, –alignIntronMin 20 –alignIntronMax 3000).[59] Featurecount (version 2.0.1) was used for quantification based on CDS features in the GFF file.[60] The raw count after Variance Stabilizing Transformation (VST) by the DEseq2 package was used for sample

clustering by Pearson correlations,[81] and the global similarity was visualised by the R package ComplexHeatmap.[82] The genes that have more than five raw counts in at least two replicates in one group were kept. For identifying the differentially expressed genes (DEGs), the R package edgeR was used.[83] Genes with a fold-change ≥ 2 and adjusted p-value (Empirical Bayes Statistics) ≤ 0.05 were considered as upregulated DEGs, while genes with an adjusted p-value (Empirical Bayes Statistics) ≤ 0.05 and fold-change ≤ -2 and were considered as downregulated DEGs. The volcano plot was generated by the R package EnhancedVolcano.[84] The gene expression levels of downregulated DEGs of different stages were obtained from Krizsán et al.,[28] and the expression heatmap was generated by R package ComplexHeatmap with row scale.[82]

The secreted proteins were predicted by SignalP (version 6.0) with default parameters.[62] The InterPro annotation was performed by InterProScan (version 5.65-97.0) with '–goterms' parameter to map the InterPro annotation to the GO terms.[61] The enrichment/depletion of the secreted proteins and genes associated with GO terms was tested by two-tailed fisher exact test (FET). The GO enrichment was performed by R package clusterProfiler,[85] the p-value cut-off was set to 0.05 with the hypergeometric test (one tailed fisher exact test), and the minimal size of genes annotated for testing was set to minGSSize=2. For the KEGG enrichment, we first found the reciprocal best hits (RBH) of the downregulated genes between *C. cinerea* Amut1Bmut1 and *C. cinerea* Okayama 7 using the "easy-rbh" module of MMseqs2 (version 13.45111).[63,86] Then the KEGG enrichment of the downregulated genes was conducted by R package clusterProfiler using *C. cinerea* Okayama 7 (ID: cci) KEGG genes database,[85] the p-value cut-off was set to 0.05, and the minimal size of genes annotated for testing was set to minGSSize=2.

Motif analyses and construction of a regulatory network

Because ChIP-Seq is not well-established for C. cinerea, we inferred regulatory information for Srr1 based on RNA-Seq data. To infer the binding motif of Srr1, six promoter datasets were established based on different upstream (or intron) regions of down-regulated DEGs (Figure 5A). We extracted the 300 bp and 500 bp upstream sequences of the start codon for the FC2 downregulated DEGs (datasets: FC2_upstream_300bp and FC2_upstream_500bp, respectively). We also isolated the complete upstream intergenic region including the first intron from FC2 downregulated DEGs (dataset FC2_intergenic_first_intron). Similarly, three datasets of FC4 downregulated DEGs were also created, named FC4_upstream_300bp, FC4_upstream_500bp, FC4_intergenic_first_intron. Analyses of motif enrichment were carried out in STREME with the following parameters: minimum motif width 6 bp, maximum motif width 10 bp, p-value cut-off 0.05, other parameters were set to default.[66]

Another independent motif prediction was performed by the online tool (https://zf.princeton.edu/) using the protein sequence of Srr1.[39] Genes with the inferred motif in FC2_intergenic_first_intron dataset were considered as the direct targets of Srr1 while others were considered as the non-direct targets. The motif distribution was illustrated for the direct targets in the FC2_intergenic_first_intron dataset with TBtools (version 2.080).[64] The network was visualized by Cytoscape (version 3.10.2) with the direct/non-direct regulatory relationships and functional group annotation.[65]

Phylogenetic and phylostratigraphic analyses

For the species tree, we selected 189 species representing the Basidiomycota with Ascomycota as outgroups. The protein files of these species were downloaded from JGI (04/2023). We used the same set of marker genes as in Merényi et al.[29]; these were identified in a reciprocal best hit (RBH) search between *C. cinerea* (CopciAB) and all proteins of the 189 species. This method was used to construct 177 clusters of single copy genes, which were aligned using PRANK (version 170427),[67] and trimmed using the TrimAL (version 1.2rev59) "-strict" approach.[68] For the supermatrix alignments with a length of at least 100 amino acids and presence of at least 75 species were required. Species tree reconstruction was performed using maximum likelihood inference (ML) in IQ-TREE (version 1.6.12).[69] For each partition, the LG+G substitution model was applied and 1,000 ultrafast bootstrap replicates were used to assess branch support.

Phylogenetic analyses of Srr1 orthologs were carried out with first identifying homologs identified through protein BLAST with an e-value cutoff of 10^{-10} in the genomes of 189 fungi. Retained homologs were aligned by mafft (version 7),[70] followed by manual inspection during which overly short (<50 aa) or divergent sequences were removed. Representatives of the most closely related C2H2-type zinc finger protein subfamily were used as an outgroup. Phylogenetic analysis was carried out in RAxML (version 8.2.12) under the CAT + WAG model with 500 rapid bootstrap replicates.[71] The sequence logos were generated by the R package ggseqlogo.[87]

For the phylostratigraphic analysis, we used the reciprocal best hit approach mentioned above. Based on the species content of these clusters, their origin was mapped to the corresponding ancestors using a custom R script.

To identify *Coprinopsis* genes that might be relevant for ballistospory, we combined three data sets. 1) RBH search between *C. cinerea* and 189 genomes mentioned above 2) Developmental transcriptome from fruiting body formation of *Coprinopsis*,[28] and 3) Developmental transcriptome of eight Agaricomycotina species analysed in Nagy et al.[40] We used Dataset 1 to characterise gene conservation among the Basidiomycota and to identify losses among the secondarily non-ballistosporic species. For screening candidate ballistospory-related genes we required 50% presence (RBH hits) among ballistosporic species, losses in at least 5 of the 8 independent secondarily non-ballistosporic clades, but at most 30 losses across the whole species tree. Dataset 2 was used to confirm the lamella-specificity of *Coprinopsis* genes. We required the highest expression in lamellae. In Dataset 3, tissue-specific expression of 1:1 orthologs was inferred by first calculating a

tissue-specificity score following Sonawane et al.[88] For tissue-specific expression we required tissue-specificity score ≥ 1 and at least four 1:1 orthologues to show lamellae or cap (because lamellae samples were not available in each species) specific expression.

QUANTIFICATION AND STATISTICAL ANALYSIS

Statistical analyses including Student's t-test, two-tailed Fisher exact test, Hypergeometric test were performed with R (version 4.3).[89] The statistical details including the test method, threshold and packages can be found in method details and main (or supplementary) figure legends.